

Portland State University

PDXScholar

Civil and Environmental Engineering Faculty
Publications and Presentations

Civil and Environmental Engineering

11-2023

Shallow-Water Habitat in the Lower Columbia River Estuary: A Highly Altered System

Will Templeton

Coastal Geologic Services, will@coastal-oceans.com

David A. Jay

Portland State University, djay@pdx.edu

Heida Diefenderfer

Pacific Northwest National Laboratory

Stefan Talke

California Polytechnic State University

Follow this and additional works at: https://pdxscholar.library.pdx.edu/cengin_fac



Part of the [Civil and Environmental Engineering Commons](#)

Let us know how access to this document benefits you.

Citation Details

Templeton, W.J., Jay, D.A., Diefenderfer, H.L. et al. Shallow-Water Habitat in the Lower Columbia River Estuary: A Highly Altered System. *Estuaries and Coasts* (2023). <https://doi.org/10.1007/s12237-023-01229-3>

This Article is brought to you for free and open access. It has been accepted for inclusion in Civil and Environmental Engineering Faculty Publications and Presentations by an authorized administrator of PDXScholar. Please contact us if we can make this document more accessible: pdxscholar@pdx.edu.



Shallow-Water Habitat in the Lower Columbia River Estuary: A Highly Altered System

William J. Templeton¹ · David A. Jay¹ · Heida L. Diefenderfer² · Stefan A. Talke³

Received: 17 November 2022 / Revised: 28 May 2023 / Accepted: 13 June 2023
© The Author(s) 2023

Abstract

Decreases in shallow-water habitat area (SWHA) in the Lower Columbia River and Estuary (LCRE) have adversely affected salmonid populations. We investigate the causes by hindcasting SWHA from 1928 to 2004, system-wide, based on daily higher high water (HHW) and system hypsometry. Physics-based regression models are used to represent HHW along the system as a function of river inflow, tides, and coastal processes, and hypsometry is used to estimate the associated SWHA. Scenario modeling is employed to attribute SWHA losses to levees, flow regulation, diversion, navigational development, and climate-induced hydrologic change, for subsidence scenarios of up to 2 m, and for 0.5 m fill. For zero subsidence, the system-wide annual-average loss of SWHA is $55 \pm 5\%$, or 51×10^5 ha/year; levees have caused the largest decrease ($54^{+5}_{-14}\%$, or $\sim 50 \times 10^5$ ha/year). The loss in SWHA due to operation of the hydropower system is small, but spatially and seasonally variable. During the spring freshet critical to juvenile salmonids, the total SWHA loss was $63^{+2}_{-3}\%$, with the hydropower system causing losses of 5–16% (depending on subsidence). Climate change and navigation have caused SWHA losses of $5^{+16}_{-5}\%$ and $4^{+14}_{-6}\%$, respectively, but with high spatial variability; irrigation impacts have been small. Uncertain subsidence causes most of the uncertainty in estimates; the sum of the individual factors exceeds the total loss, because factors interact. Any factor that reduces mean or peak flows (reservoirs, diversion, and climate change) or alters tides and along-channel slope (navigation) becomes more impactful as assumed historical elevations are increased to account for subsidence, while levees matter less.

Keywords Habitat · River-estuary · Shallow-water habitat area · Tidal-fluvial interactions · Tidal river · Salmonids

Communicated by Carles Ibañez Martí

✉ William J. Templeton
will@coastal-oceans.com

David A. Jay
djay@pdx.edu

Heida L. Diefenderfer
Heida.Diefenderfer@pnnl.gov

Stefan A. Talke
stalke@calpoly.edu

¹ Department of Civil and Environmental Engineering, Portland State University, Portland, USA

² Coastal Sciences Division, Pacific Northwest National Laboratory, Sequim, WA, USA

³ Department of Civil and Environmental Engineering, California Polytechnic State University, San Luis Obispo, CA, USA

Introduction

Seaward migrating salmonids and other fauna use tidally influenced shallow-water habitat area (SWHA) in river-estuaries for feeding and protection from predation. As in most major US estuaries and tidal rivers (Hughes et al. 2005), wetland area has been greatly reduced in the Lower Columbia River and Estuary (LCRE). To support fish population recovery, restoration of wetlands is now a major management focus. Nonetheless, restoration can be challenging because multiple factors, including bathymetric and hydrological changes, alter wetland extent but also the hydrodynamic response of the system, including tides and mean water levels (Helaire et al. 2019; Hoitink & Jay 2016; Jay et al. 2011; Talke & Jay 2020). Moreover, estuarine restoration presupposes knowledge of desirable system states (Thom et al. 2010). The requisite knowledge includes mapped data such as the historical location and extent of wetlands, biogeographic information such as species

distributions, and dynamics of historical currents, water levels, salinity, and temperature, but also an understanding of how and why processes and landforms have changed and current trends (Gann et al. 2019; Palmer et al. 2016). Our knowledge of past estuarine conditions and processes is generally limited, though recovery of historical water level datasets has become more widespread (see, e.g., Talke and Jay 2013; Latapy et al. 2022). It is necessary to design measurable indicators of past and present states to evaluate the degree and importance of changes, and to assess whether current management strategies for salmon recovery are addressing the most important factors causing habitat loss.

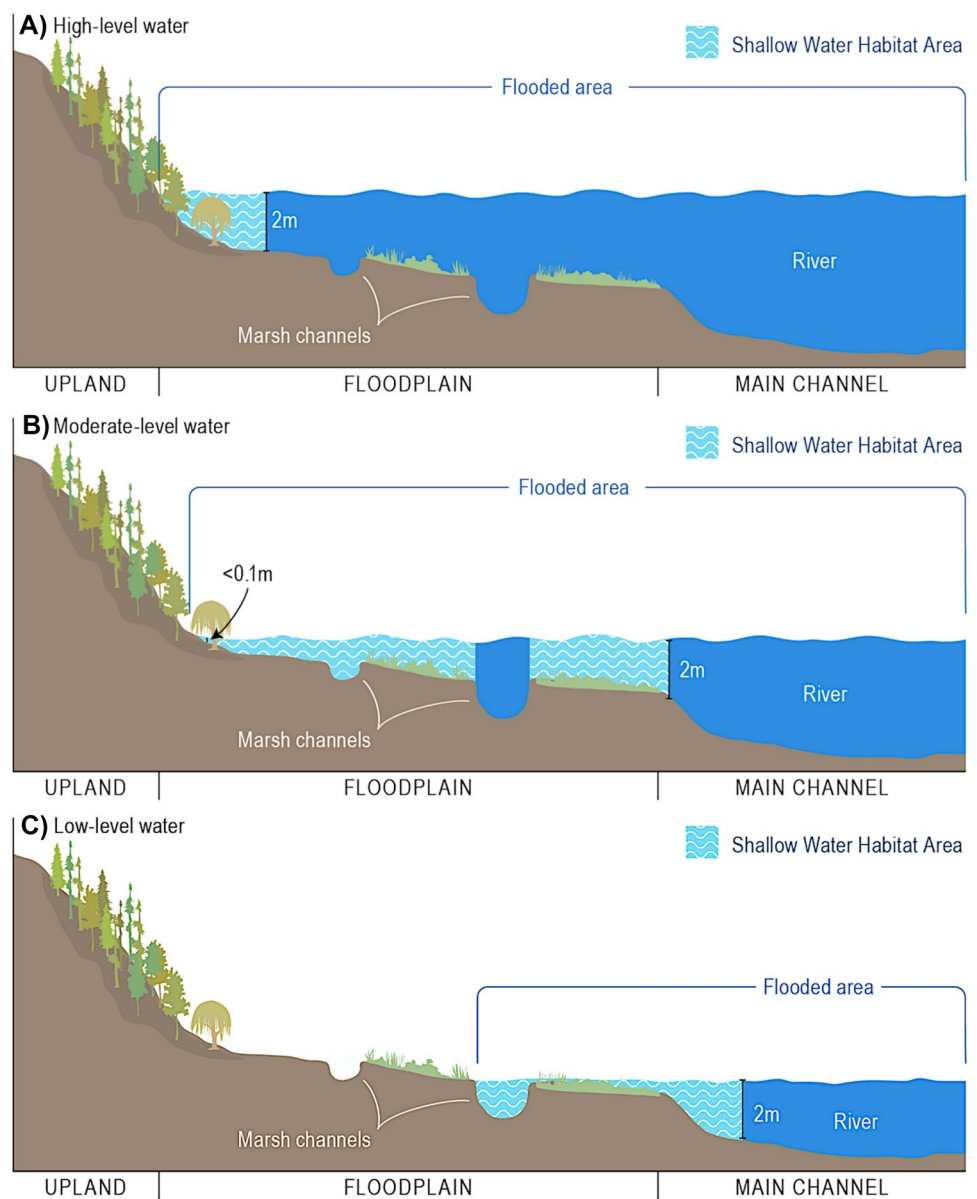
SWHA is important to the survival of juvenile salmonids migrating seaward, because they use this habitat to rest, feed, and undergo smoltification (Johnson et al. 2015; Roegner et al. 2016; Sather et al. 2016). A large fraction of potential SWHA in the LCRE has been lost since the 1800s, and this has been implicated in the decline of threatened and endangered populations (Bottom et al. 2005). We say “potential” here, because the inundation that creates SWHA is dependent on river flow, tides, and other factors, not only upon connectivity between the habitat and the larger system. Because of its importance, restoration of SWHA is a primary reason for the ongoing restoration of wetlands by the Columbia Estuary Ecosystem Restoration Program (Diefenderfer et al. 2016; Ebberts et al. 2018). The program restored nearly 9% of recoverable floodplain by the end of 2021 (Littles et al. 2022), and our work provides a basis for future analyses of the SWHA effects of restoration as the impacts of sea level rise and other climate-change-induced hydrological changes become clearer.

Characteristics of inundation, such as variable frequency, magnitude, duration, and spatial coverage, are used to define wetlands and are amongst the most critical for wetland functions (Bunn and Arthington 2002; Strayer and Findlay 2010; Wohl et al. 2015). Inundation, as approximated from water levels, is also one of few hydrologic processes with sufficient historical data to permit detailed analysis of past system conditions, and SWHA is an inundation metric based primarily on water levels. SWHA for juvenile salmon in tidal rivers and estuaries has been defined as the area inundated to a depth between 0.1 and 2 m with a velocity $< 0.3 \text{ ms}^{-1}$ (Bottom et al. 2005). Consequently, SWHA is a function of spatially and temporally varying water depth and velocity. Here, we evaluate SWHA in terms of depth, given the dearth of velocity measurements in wetland areas. We evaluate SWHA for the middle and upper estuary through the tidal river (the most landward 213 river kilometers [rkm] of the system), because the higher high water (HHW) models informing our SWHA evaluation are not suited for predicting conditions near the river mouth where the effects of coastal forcing, local winds, waves, and salinity intrusion are better represented by hydrodynamic models.

Conceptually, SWHA changes with water level relative to local topography (Fig. 1). During flood conditions, large parts of the floodplain are inundated to > 2 m depth, and steep topography in the incised valley of the Columbia River sharply reduces SWHA (Fig. 1A). With moderate water levels, more of the floodplain is covered to < 2 m depth (Fig. 1B) than during high water levels (Fig. 1A). For low river flows, most of the floodplain is not inundated, thereby limiting SWHA (Fig. 1C). Comparison of the three situations emphasizes that, as water levels rise, SWHA shifts from low-lying areas near the channel, up the floodplain to higher terrain nearer the upland. The location of wetlands along the estuary–tidal river gradient also matters—seasonal high flows may lead to only slightly elevated water levels (Fig. 1B) in the estuary but much high-water levels in the tidal river (Fig. 1A), because the range of water level variation is much larger upriver. Finally, levees in the higher parts of the floodplain reduce SWHA and leave remaining potential SWHA at lower elevations closer to the thalweg. As we will see, reduced flows have partially compensated for leveed SWHA habitat high in the floodplain, especially in the tidal river. Specifically, low-elevation floodplain that would previously have been flooded to > 2 m with spring snowmelt is now sometimes SWHA under the prevailing lower spring flow regime typical of rivers regulated for hydropower production and other uses (Poff et al. 1997).

This study uses historical water level data to construct a statistical model (per Kukulka and Jay 2003a, b, henceforth KJ2003a,b; and Jay et al. 2011) of HHW for each river-kilometer between rkm21 and the head-of-tide at rkm234, from 1928 to 2004. These HHW values are then used to estimate daily SWHA in the oligohaline and freshwater parts of the LCRE, and to explore the reasons for changes in SWHA. The long timescale of our analysis allows evaluation of how spatially variable increases in tides and reduction in river slope since the 1920s (e.g., Helaire et al. 2019; Jay et al. 2011; Talke et al. 2020) impact SWHA. Similarly, the system-scale approach enables a comparison/contrast between fluvially dominated reaches and those more influenced by tides. Thus, this analysis broadens the spatial scope of prior SWHA analyses: KJ2003a,b (between rkm50 and rkm90, from 1974 to 1998), and Bottom et al. (2011; between rkm83 and rkm120, from 1925 to 2004). The current study uses updated bathymetry and topography derived from recent LiDAR and hydrographic surveys and incorporates historical water level data from the 1940s that were not available to prior studies. For each river kilometer, daily values of SWHA for 1928–2004 are summed by time period and over the system reaches (Fig. 2). SWHA changes for each season (freshet, non-freshet, and annual) are then attributed to five factors: levees, flow regulation, flow

Fig. 1 Typical distributions of SWHA over the floodplain for **A** high flows and water levels, **B** moderate flows and water levels, and **C** low flows and water levels. The SWHA part of the flooded area is between 0.1 and 2.0 m deep



diversion, navigation channel development, and climate change. Uncertainties are analyzed, and the effects of assumed subsidence on the analysis are examined.

Setting

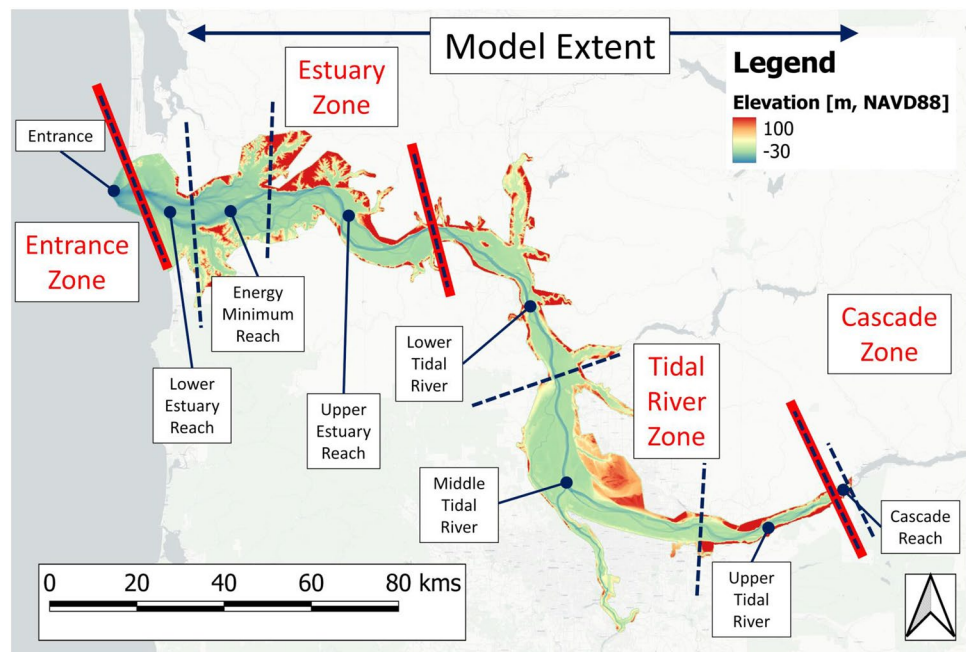
The LCRE extends 234rkm from the Pacific Ocean to the head-of-tide at Bonneville Dam (Fig. 2). The system is divided into four zones and eight reaches based on topography, salinity intrusion, the balance of tidal and fluvial forcing, and analyses of vegetation throughout the system (Jay et al. 2016; Fig. 2; Table 1). Zone boundaries are related to the predominant sources of energy dissipation and topographic features, like constrictions. River flow is

the dominant energy source in the more landward reaches, while tides and coastal processes predominate in reaches near the ocean. Simenstad et al. (2011) reached similar conclusions regarding classification, using a somewhat different methodology.

Hydrology, Geomorphology, Tides, and In-channel and Floodplain Infrastructure

More than half of the historical (early 1800s) LCRE floodplain has been isolated from the fluvial system by levees, earthen constructions that entirely or mostly prevent inundation of the areas they encompass. In the Lower Columbia River Estuary (LCRE), most levees are directly adjacent to the main channel even under low river-flow conditions,

Fig. 2 LCRE zones and reaches based on Jay et al. (2016), with elevations shown as a blue (main channel substrate elevation) to green (shallow-channel low elevation) to red (higher elevation floodplain) colormap. Reaches are delineated by dashed black lines, while zones are separated by red lines. The total extent of the study area consists of the six most landward reaches, from the Energy Minimum to the Cascade. The Lower Estuary Reach is immediately west of the study area



isolating the entire adjacent floodplain from inundation and limiting the potential extent of SWHA. Hydrologic change is another primary factor that alters SWHA. Mean annual flows are 15–17% below pre-1900 levels, primarily due to climate change and water withdrawal for agriculture (Jay and Naik 2011b; Naik and Jay 2011a, b). Additionally, maximum spring freshet flows are down 40–45% on average, mostly due to flow regulation and irrigation. Autumn and winter flows have increased in compensation. Since the nineteenth century, these flow changes have increased average wintertime water levels in Astoria (rkm25) by

0.03–0.04 m, and decreased May–July water levels by 0.05–0.15 m (Talke et al. 2020); further upstream in the Portland/Vancouver region (rkm170), much larger average decreases of ~1–4 m have occurred during the freshet season (Helaire et al. 2019). The seasonal shifts in hydrologic change interact with other factors, especially the levee system and changing tides. The levee system confines high flows, raising water levels throughout most of the system, relative to a connected system with the same channel depth (Helaire et al. 2019), while tidal range varies inversely with discharge in the tidal river.

Table 1 Zones and reaches of the LCRE, based on Jay et al. (2016). SWHA calculations were made for the six reaches from rkm21 to rkm234

Zone	Reach	Rkm range	Features
Entrance	Entrance	0–5	<ul style="list-style-type: none"> • Dominated by waves and tidal processes • Sparse vegetation data
Estuary	Lower Estuary	5–21	<ul style="list-style-type: none"> • Affected primarily by tides and salinity intrusion • Landward boundary roughly corresponds to upstream limit of salinity intrusion during typical spring high flows
Estuary	Energy Minimum	21–39	<ul style="list-style-type: none"> • Widest part of estuary • Tidal emergent wetlands have high vegetative cover with relatively low species diversity
Estuary	Upper Estuary	39–87	<ul style="list-style-type: none"> • Convergent cross-section with increasing fluvial influence • Fluvial influence strong enough that tides are considerably damped despite convergence
Tidal River	Lower Tidal River	87–139	<ul style="list-style-type: none"> • Steep topography • Single channel through most of the reach
Tidal River	Middle Tidal River	139–196	<ul style="list-style-type: none"> • Extensive historical floodplain through confluence of Willamette and Columbia Rivers • Seasonal-fluvial processes play large role
Tidal River	Upper Tidal River	196–229	<ul style="list-style-type: none"> • Cliffs on either side of river up to base of Bonneville landslide • Tides are small
Cascade	Cascade	229–234	<ul style="list-style-type: none"> • Steep bed slope due to the Bonneville landslide; high turbulence • High seasonal mean water level fluctuations due to river discharge

LCRE tides have evolved due to changing morphology and river flows (e.g., Al-bahadily 2020; Helaire et al. 2019; Jay et al. 2011, 2015, 2016; Talke et al. 2020). The largest changes have been due to development of the Federal Navigation Channel (FNC), which extends from the ocean to Vancouver and Portland Harbor (Helair et al. 2019; Jay et al. 2011, 2016; Sherwood et al. 1990). The FNC includes 17 km of stone entrance jetties, an 18-m-deep entrance channel, a 13-m-deep channel from rkm5 to Vancouver (rkm170), and a series of stone and timber pile dikes that direct flow into the navigation channel. Compared to the nineteenth century conditions, the FNC has straightened and approximately doubled the thalweg depth of the system, decreasing frictional effects and reducing mean water levels, though pile dikes introduce friction and prevent an even greater decrease in water levels (Helair et al. 2019, 2020; Jay et al. 2011). Reduced friction has increased tidal ranges in the reach between Astoria (rkm25) and Quincy (rkm87) on the order of 5–20% (Helair et al. 2019; Talke et al. 2020). Tidal changes are large upriver, especially for high river-flow levels (Helair et al. 2019; Jay et al. 2011). Off-channel areas and wetlands have been filled as a result of dredged material disposal and for development, and islands have been constructed to help train the flow and retain dredged material (Marcoe and Pilson 2017; Sherwood et al. 1990). Overall, lower low water (LLW) levels have decreased more than HHW levels have increased, reducing the mean water level (Helair et al. 2019; Jay et al. 2011). Changing river flow impacts tides, seasonally, and the largest increase in tidal amplitudes has occurred during the spring freshet (Talke et al. 2020), modestly counteracting decreased flows in some reaches, in terms of providing inundation.

System Ecology and Habitats

The LCRE, and particularly its vegetated habitats including both native and introduced plants (Borde et al. 2020), provides important habitat for a large number of animals (Callaway et al. 2012; Johnson and Simenstad 2015). The many salmon and trout stocks represent culturally and economically important species dependent on the LCRE food web (Blumm 2002; Lichatowich et al. 2018; Naiman et al. 2012; Pulwarty and Redmond 1997; Waples et al. 2008). Juvenile salmonids require off-channel LCRE habitat with low salinity and water depths in a specific range, during their migration to the ocean (Bottom et al. 2005). These habitats can provide access to food, refuge from higher-velocity flows, and cover from predation (Johnson et al. 2015; Maier and Simenstad 2009; Roegner et al. 2010). Development of the LCRE and the Columbia River Basin since the middle of the nineteenth century has affected flow, water temperature, connectivity between the main channel and side channels and floodplains, sediment supply, and salinity intrusion and

stratification, all of which may alter the structure or function of habitats in the river (Harding et al. 2020; Jay et al. 1990; McKeon 2022; Naik and Jay 2011a, b; Roegner et al. 2021; Scott et al. 2023; Sherwood et al. 1990; Simenstad et al. 1992; Templeton and Jay 2013). Plant distribution itself has been widely modified, with conversion from wetland to agriculture and urbanization, ecological impacts of hydrologic change, and floodplain forest harvest and management (Borde et al. 2020; Ke et al. 2013; Thomas and Bell 1983). Since the 1870s, herbaceous wetland area decreased from 35,466 to 11,381 acres (68%), while forested and shrub-scrub decreased from 39,439 to 12,289 acres (69%; Marcoe and Pilson 2017). Virtually all of this loss is due to the levee system, filling, and urban development. These wetland losses have strongly affected habitat availability for migrating and temporarily resident juvenile salmonids (Bottom et al. 2011; Johnson et al. 2015), but SWHA has also been altered by changing hydrology and tides.

Topographic change is an important consideration in a study with a 75 + yr scope, quite aside from the presence or absence of levees. Sediment accretion rates have been found to be positive in extant reference wetlands in the study area, counteracting subsurface subsidence (Diefenderfer et al. 2021). Also, some elevation changes in wetlands have occurred because of tectonic processes, particularly near the coast where uplift occurs (Burgette et al. 2009; Miller et al. 2018; Talke et al. 2020). Larger changes have been produced by isolation of floodplains by levees, and the subsequent elevation reduction due to spatially variable subsidence. By comparing isolated and connected areas of the floodplain, Cannon (2015) estimated a range of subsidence, with 0.4 m near the Lewis River and 2.9 m near rkm80; however, 2.9 m is more than twice the level of subsidence as the next nearest measurement (1.4 m) and is recognized as an anomaly explained by local conditions. Median subsidence was 0.80–0.89 m over the entire historical period since levees were built. Similarly, Diefenderfer et al. (2008) found evidence of a ~0.7 m difference between an adjacent un-leveed wetland and leveed pasture. Applying the LiDAR correction factor, the likely median subsidence is ~0.5–0.6 m, not all of which has occurred since 1928. Diefenderfer et al. (2018) showed that microtopographic relief, an important aspect of wetland complexity that affects the spatial pattern and location of SWHA at any given river stage, was reduced in leveed agricultural areas. Floodplain isolation has resulted in decreases in groundwater levels, soil consolidation, decomposition of organic materials that are no longer replenished, and agricultural activities such as grazing that can further compact the soil (Cannon 2015; Tornqvist et al. 2008). Although most of the LCRE upstream of Astoria (rkm 25) has likely subsided, some along-channel and urban parts of the floodplain have been filled. Causes of filling include land reclamation, disposal of dredge materials, and natural

events such as catastrophic debris flows and subsequent sedimentation in the LCRE following the eruption of Mt. St. Helens in 1980 (Simenstad et al. 2011; Zheng et al. 2014). Thus, while modern topography is reasonably well defined (see below), historical topography is uncertain; therefore, we consider the influence of assumed subsidence and infill on our results.

Development of the Federal Columbia River Power System (FCRPS) has greatly affected water levels through upstream flow regulation for flood control and power generation, and water withdrawal for agriculture. Even though irrigation withdrawal largely occurs through FCRPS management, it is evaluated here as a separate factor because it results in a net loss of water supplied to the LCRE, unlike power generation and flood control. The FCRPS and, to a lesser extent to date, climate change, have greatly altered the annual runoff hydrograph for the mainstem Columbia and its LCRE tributaries, e.g., Willamette, Lewis, and Cowlitz Rivers (Jay and Naik 2011; Naik and Jay 2005, 2011a).

Methods

This study expands on the KJ2003a,b approach for estimation of SWHA. Daily SWHA is estimated from HHW and system hypsometry. Specifically, historical tidal data are used to construct a statistical model of HHW for every river kilometer (rkm) of the LCRE between rkm21 and the head-of-tide at rkm234 for the period 1928 to 2004. A statistical model was employed, in lieu of a numerical model, given a lack of an appropriate hydrodynamic grid for floodplain areas, and the computation and memory costs of running and storing model outputs for near-centennial time periods and multiple scenarios. The domain modeled includes the six most landward LCRE reaches (Fig. 2). Numerous factors influence water levels in the LCRE, including bathymetry and topography, tides, river discharge, and coastal processes such as coastal upwelling and storm surges (Helaire et al. 2020), and could potentially be included in our statistical models. Based on KJ2003a,b and Jay et al. (2016), HHW is modeled using the following forcing terms: river inflow from the Columbia River (2) and Willamette River (3), Coastal Upwelling Index (CUI) (4), non-linear tide-flow interaction (5), and datum offset (1); numbers in parentheses refer to the terms in Eq. 1:

$$HHW = \underbrace{a_{0k}}_1 + \underbrace{a_{1k}Q_B^m}_2 + \underbrace{a_{2k}Q_{WR}^n}_3 + \underbrace{a_{3k}CUI}_4 + \underbrace{a_{4k}\left(\frac{T_{R,H}^s}{(1+Q_B+Q_{WR})^r}\right)}_5 \quad (1)$$

where:

Q_B = Daily mean Columbia River flow at Bonneville Dam or the Beaver Army Terminal, 1000s of m³/s

Q_{WR} = Daily mean Willamette flow at Portland, 1000s of m³/s

CUI = Daily Coastal Upwelling Index, in 10 m²/s, positive for upwelling (Bakun 1973)

$T_{R,H}$ = Greater diurnal tidal range (m), or HHW-LLW, at Hammond or Astoria

a_{ik} to a_{ik} = Regression parameters for each station and model

k = Index for channel stations; varies with modeling time periods (MTPs)

s = Tide-flow interaction exponent; varies with location and model

m = Columbia flow exponent; varies with location and model

n = Willamette flow exponent; varies with location and model

r = Second tide-flow interaction exponent; varies with location and model

a_{ok} = Datum offset

The model describes the effects of river flows and coastal processes on water levels in the second through fourth terms, and the effect of nonlinear interactions between flows and tides in the fifth term. The constant first term accounts for datum offsets. Future modeling efforts could include atmospheric effects in more detail, assuming adequate availability of historical pressure data or a proxy thereof, but the effects are likely small compared to the effects of river flows, tides, and coastal processes, especially in the more landward parts of the system. Seaward of rkm90, the second term of the regression uses flows at Beaver Army Terminal, the third term is not used, and the fifth term uses flows at Beaver Army Terminal and does not include flows for the Willamette River. Landward of rkm90, the second term of the regression uses flows at Bonneville Dam, the third term is included, and the fifth term uses flows at Bonneville Dam and includes flows for the Willamette River.

Our approach differs from Jay et al. (2016) in that the coastal forcing variable (Coastal Upwelling Index) is averaged on a year-day basis (every Julian day during the record is averaged and applied to every year) from 1967 to 2011 and applied to all modeling periods, because the relevant forcing data are not available before 1967. Jay et al. (2016) found coastal forcing to be relatively important in the estuary up to about rkm30, but increasingly irrelevant further landward. Given a study area that is mostly upstream of this point, the climatological approach used here for incorporating coastal effects in the model is appropriate.

The HHW model (Eq. 1) is applied at water level stations throughout the system to estimate coefficients and exponents, as listed in the Supplement (Tables S1 to S3). Model coefficients and exponents are interpolated between water level stations to derive HHW models at 1 km intervals

for the entire system. SWHA, defined in hectares (ha) at HHW, is then determined from hypsometry. The assumptions involved in using this approach to estimate SWHA are that: (1) entrance tidal range (from Astoria or Hammond) and river flow are the primary drivers of tidal-fluvial water levels, with other variables playing a secondary role; (2) tide gauges at channel locations provide reasonable estimates of water levels over the floodplain; (3) the water surface slope across the floodplain is smallest at HHW, making HHW the most useful water level statistic; (4) time lags in inundation and slopes across the floodplain are irrelevant for SWHA estimation; (5) once-daily inundation is sufficient to render a wetland functionally useful as habitat; and (6) tidal properties and water surface-slope vary slowly in space, so that the spatial interpolation of the coefficients is valid. During high-flow periods, there is very little difference in the tidal river between LLW, mean water level (MWL), and HHW in the tidal river landward of Quincy at rkm87, because tidal ranges are small under these conditions. Thus, estimation of SWHA from a HHW model is most accurate during high flow periods when inundation and SWHA are extensive. As a qualitative tool for evaluating historical change, this approach is useful for all flow conditions. However, SWHA is strictly an areal measure, not a measure of quality; thus, SWHA may have different utility in different habitats, different seasons, and different eras.

We determined SWHA for a series of scenarios involving the presence/absence of levees and naturalized, adjusted, or observed flows (Table 2); we refer to these as the six basic scenarios. SWHA for each scenario was summed over the freshet season (May through July), the rest of the year, and the full year (per KJ2003a,b; Bottom et al. 2005). GIS data for levees were obtained from the “human cultural features, infrastructure, and modifications” layer in the Ecosystem Classification (Simenstad et al. 2011), a tool developed for use by the Columbia Estuary Ecosystem Restoration Program (Littles et al. 2022). Observed flows are instrumental records available on a daily basis, or estimates of the flow that would have been observed had instruments been in place; the latter are derived by flow routing (Naik and Jay

2005, 2011b). Adjusted flows are hypothetical flows that would have occurred without flow regulation and reservoir storage; these flows are still reduced by irrigation depletion. Naturalized (or virgin) flows are the hypothetical flows that would have occurred if there were no European settlements; i.e., they have been corrected for flow regulation, reservoir storage, and irrigation depletion. The naturalized flow calculation does not account for changes in land use such as agriculture, urban development, and forestry, though changes in evapotranspiration may have changed Columbia River flows by 1–2% on an annual average basis, with a larger influence in some seasons (Matheussen et al. 2000). These changes are small relative to observed changes since the nineteenth century, which include decreases in annual average flow and peak spring flow of ~15% and >40%, respectively.

Data

Model forcing data were taken from a variety of sources, including (1) river flow data for the Columbia River at The Dalles (1878–present) and Beaver Army Terminal (1991–present), and for the Willamette River at Portland (1972–present) from the USGS; (2) river flow data for the Columbia River at Bonneville Dam (1949–present) from the BPA; (3) tidal range at Hammond (rkm11) and Astoria Tongue-Point (rkm29), as predicted using T_Tide (Pawlowicz et al. 2002) from time series from the National Oceanographic and Atmospheric Administration (NOAA); and (4) daily averaged CUI as provided by NOAA (1967–present) and averaged by year-day over all annual periods in the record and applied to the modeling time periods (MTPs) defined below.

Measured HHW values at tide gauges located throughout the system (Table 3) were used as a response variable to determine the coefficients of Eq. 1 using robust multiple linear regression; the forcing data were used as predictor variables. Tidal data were available from more than 20 NOAA stations along the system in 1940–1943 that we digitized; most have 20 months of data or more. Relatively comprehensive water level data have been collected since 1980, but data from between 1950 and 1980

Table 2 SWHA basic scenarios evaluated for 1928 to 2004 where connected conditions represent floodplain connection assuming levees do not exist, and isolated conditions represent floodplain isolation by the existing levee system

Scenario	Levee condition	Flow
1	Connected (without levees)	Naturalized
2	Connected	Adjusted
3	Connected	Observed
4	Isolated (with levees)	Naturalized
5	Isolated	Adjusted
6	Isolated	Observed

Table 3 Water level data used in regression models where MTP represents model time periods

Station	Rkm	Availability	Model period(s) used
North Jetty	2.6	1982	MTP3
Fort Stevens	13.2	1940–1943, 1981	MTP1,3
Hammond	14	1982–1988, 2011–2014	MTP3
Astoria	29.22	1925–date	MTP1-3
Altoona	39.1	1940–1942	MTP1
Skamokawa	53.6	1940–1942, 1978, 1986–date	MTP1-3
Cathlamet	63.57	1940–1942	MTP1
Wauna	67.4	1940–1942, 1972–1979, 1986–date	MTP1-3
Eagle Cliff	81.97	1940–1942	MTP2
Beaver/Quincy	87	1991–date	MTP3
Stella	90.6	1940–1942	MTP1
Longview	106.94	1940–1942, 1986–date	MTP1,3
Rainier	109.7	1971–1981 (gaps)	MTP2
Kalama	120.7	1940–1942	MTP1
Columbia City	134.3	1971–1981	MTP2
St. Helens	138.6	1940–1943, 1991–date	MTP1,3
Willow Bar	154.3	1940–1942	MTP1
Kelley Point	163.45	1940–1942	MTP1
Vancouver	171.5	1940–1942, 1972–date	MTP1-3
Ellsworth	181.05	1940–1942	MTP1
Washougal	190.5	1940–1942	MTP1
Reed Island	198	2007–2009	MTP3
Prindle	217.6	1940–1942	MTP1
Warrendale	229.3	1940–1942, 1971–1988	MTP1,2
Bonneville	233	1966–2016 (gaps)	MTP2,3

are sparse. Only one tide gauge, NOAA station #9439040 at Tongue Point (Astoria, OR, 1925–date) is available for the entire period. Data used are identified in Table 4; see Helaire et al. (2019) and Talke et al. (2020) for sources of archival data and information about the history of tidal measurements in the LCRE. To use the available water level data as efficiently as possible, regression models were developed for three MTPs: (period 1) 1928 to 1959, (period 2) 1960 to 1979, and (period 3) 1980 to 2004. Because of data availability, different stations were used during each period. Analyses were not carried out after 2004, because the naturalized and adjusted flow estimates of Naik and Jay (2005, 2011b) do not extend beyond 2004. BPA published

naturalized flows for some stations through 2008, but not all stations needed for this analysis; no-post-2008 data are available. Also, floodplain-ecosystem restoration begun about 2004 complicates later estimation of SWHA, because associated levee breaching (Littles et al. 2022) alters topography and hydrological connectivity between the floodplain and the mainstem river. Though relatively little breaching occurred before 2013, roughly 30 km² of floodplain was reconnected by 2021 (Littles et al. 2022). Thus, our evaluation of levees represents the largest (pre-restoration) effect on SWHA. Analyses were not conducted prior to 1928, the beginning of the adjusted flow record at Bonneville Dam.

Table 4 Daily data for factors that affect water levels in the LCRE

Factor	Availability
Columbia River Discharge at Bonneville Dam	1878–date, routed before 1949
Willamette River Discharge at Portland	1878–date, routed before 1972
Columbia River Discharge at Beaver Army Terminal, OR	1878–date, routed before 1991, ex. 1968–1970
Coastal Upwelling Index	1967–date, climatologically averaged from 1967 to date for and applied to all periods
Greater Diurnal Tidal Range at Hammond	1925–date

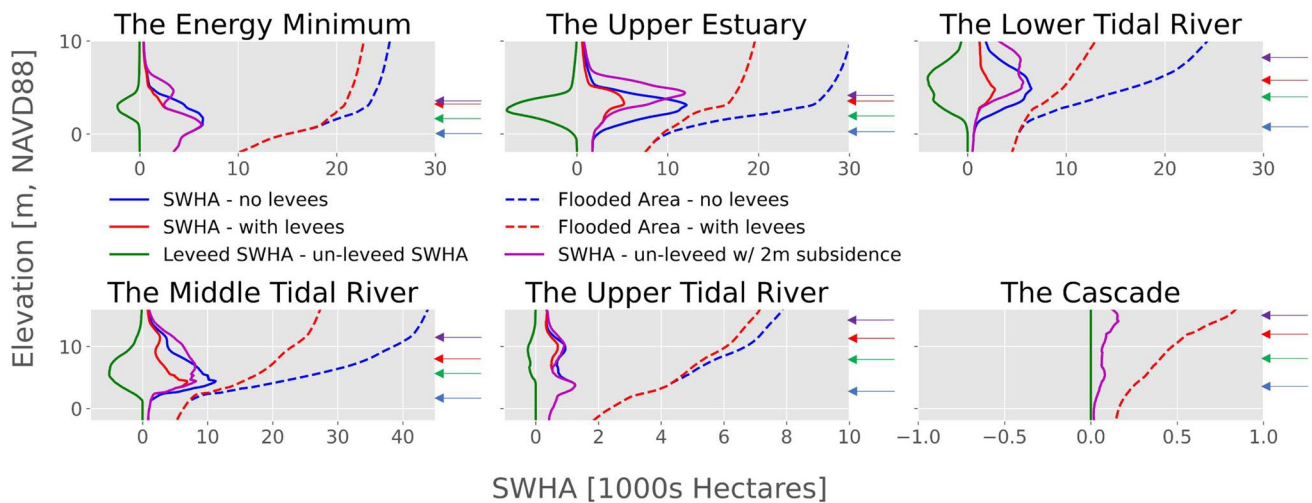


Fig. 3 SWHA hypsometric curves (solid lines) and flooded area (dotted lines), by reach. SWHA hypsometry is shown for connected (no levees) versus isolated (leveed) topographic scenarios, for the difference between the two, and for historical conditions (purple line) assuming a uniform 2 m subsidence; 2 m subsidence is much larger than has occurred on average but illustrates the effect of changing

hypsometry on SWHA. Leveed areas do not constitute SWHA, even when flooded. Arrows at right, from low to high elevations: Columbia River Datum (extreme low water, blue); the modern 2-year flood level (green); the 1933 flood (a large flood early in our analysis period, red); and the highest flood since 1850 (1894; purple)

Modeling Details

SWHA is determined by modeling HHW for each calendar day and scenario in each reach and estimating inundated area from the hypsometric curve for the reach, 1928–2004, taking into account the SWHA 2-m depth limit. A hypsometric curve gives floodplain area as a function of water level for a reach. Hypsometry for each reach is determined by summing hypsometric curves determined from a digital terrain model (DTM) at 1rkm intervals over the reaches shown in Fig. 2. The DTM used for the analysis was the modern 2010 Lower Columbia River Digital Terrain Model developed by the USACE (USACE 2010). Separate hypsometric curves are defined for isolated and connected conditions. SWHA curves are then estimated, taking into account the SWHA depth limit of 2 m (Fig. 3). As water levels rise, SWHA first increases as water spreads out over the floodplain, but then decreases as more area is inundated above the upper threshold of SWHA (2-m depth); see also Fig. 1. The difference in SWHA between connected and isolated conditions (Fig. 3, leveed SWHA–un-leveed SWHA) is the loss of potential SWHA due to levees; this loss is concentrated in the Upper Estuary, Lower Tidal River, and Middle Tidal River reaches. SWHA for connected conditions is found between the extreme low water and historical flood levels (Fig. 3, arrows). Correcting for subsidence considerably alters the elevation distribution of SWHA. Maximum historical SWHA was likely at an elevation somewhere between the bounding lines for connected conditions, and for connected

conditions with 2 m subsidence. These higher floodplain elevations were reached by historic floods (1933 and 1894 arrows); modern floods do not reach those elevations (see also Helaire et al. 2019).

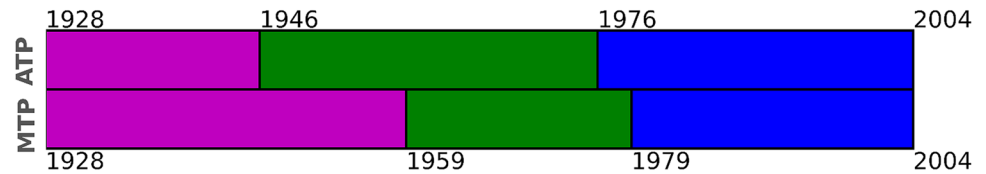
The SWHA determined for each reach and each day is then summed over the year and over longer periods, defined below. A major purpose of this work is to evaluate habitat changes affecting juvenile salmonids, and there is strong seasonal variability in salmonid use of SWHA, with the spring “freshet season” (May to July) being the most important (Bottom et al. 2005). Following KJ2003a,b, the freshet season is, therefore, distinguished from the remainder of the year (denoted as “non-freshet season”), and SWHA is summed within the year and interannually by season.

Attribution

We use a process we call “attribution” to divide the total loss of SHWA amongst the five major factors (“attribution factors”) or stressors that have altered water levels and inundation in the system:

- Levees and associated conversion of estuarine wetlands to other uses
- Development and operation of the Federal Columbia River Power System (FCRPS)
- Development of the Federal Navigation Channel (FNC)
- Irrigation diversion

Fig. 4 Relationship between the attribution time periods (ATPs) and modeling time periods (MTPs)



- Climate change effects on the seasonal hydrograph and total annual flow

These factors were chosen because they are the largest factors that alter tidal range and river flow, the major predictor variables in Eq. 1. Models using these variables provide a reasonably accurate representation of LCRE water levels (Helaire et al. 2019; KJ2003a,b; Jay et al. 2011, 2016). Additional climate change effects such as relative sea level rise are not considered, because historical changes have been small—about 0.06 m in Astoria since the mid-nineteenth century (Talke et al. 2020). Moreover, sea-level rise effects on water level decrease in the upstream direction, particularly during high river flow conditions (Helaire et al. 2020), and MWL in the tidal river has actually decreased since 1900 due to navigational improvements and flow reductions. The effect of the latter can reduce spring freshet water levels by up to 3–4 m (Jay et al. 2011, 2016; Helaire et al. 2019). The effect of climate change, therefore, is evaluated by comparing SWHA for naturalized Columbia and Willamette River flows between historical (pre-1900) and modern conditions, with all other factors (i.e., tides, hypsometry, and coastal processes) constant.

Attribution of SWHA losses over the 1928–2004 period is based on a total of more than 20 scenarios in which topography and forcing variables are systematically varied, e.g., the effect of levees can be estimated by comparing leveed (disconnected wetland) and un-leveed (connected wetland) scenarios, keeping other factors constant. Attribution further requires the estimation of SWHA during different attribution time periods (ATPs) to evaluate SWHA changes and their causes over the past century. The time periods are:

- ATP1 (essentially pre-alteration, except for some irrigation withdrawal, early navigational development and some tributary dams, 1928–1945)
- ATP2 (FCRPS under development and irrigation in place, plus an 11-m deep navigation channel; 1946–1975)
- ATP3 (the modern, altered system with a 13-m deep navigation channel; 1975–2004)

Each ATP is analyzed using the three flow scenarios: naturalized, adjusted, and observed flows. The ATPs were chosen to provide an understanding of historical changes; they cross MTP boundaries, which were chosen to make efficient use of data (Fig. 4). We note that most LCRE levees were

constructed between the 1880s and 1930s, so were largely in place during ATP1. To evaluate the effect of levees, scenarios with and without levees (disconnected and connected habitat) were used in all ATPs. See the Supplement for details of how attribution was implemented for each attribution factor.

The above list of factors causing changes in SWHA is not exhaustive—factors with smaller impacts such as deforestation and changing ocean tides are not included. Nor, with the exception of levees, does the present study consider changes that occurred before 1928, because we do not have sufficiently high-quality, system-wide water level data to merit an earlier MTP. Also, increases in SWHA due to restoration efforts are not considered, because we lack an appropriate set of hypsometric curves, which would need to account for year-to-year changes in restored habitat since about 2004.

Our attribution strategy is to calculate the total loss of SWHA and then compare the modern system to the *unaltered system*, before it was altered by the five attribution factors. Factors are varied one at a time. For our purposes, the unaltered system assumes connected topography, no upstream irrigation diversion, no FCRPS, and no FNC (i.e., unaltered tides and mean water level); SWHA for the unaltered system is the *unaltered SWHA*. The unaltered SWHA for each reach is calculated using ATP1 tides, naturalized flows, and connected topography; the model used for comparison depends on the factor being evaluated against the *unaltered system*. The *total loss of SWHA* is the difference between unaltered SWHA and SWHA estimated for ATP3 using observed flows, modern tides, and isolated topography for each reach. While the various components of the total loss can be estimated by individual attribution factor (levees, FCRPS, FNC, irrigation, and climate change), factors interact or overlap, so that the total loss is not equal to the sum of the individual losses by factor, contributing to the overall uncertainty level. Finally, subsidence, poorly known in this system, will emerge as the most important factor driving uncertainties in SWHA losses and their attribution.

The above strategy was augmented for the FCRPS scenario, because its effects overlap so extensively with the levee system. Hence, FCRPS impacts on SWHA were evaluated with both the connected (un-leveed) and disconnected (leveed) hypsometry. Finally, our attribution procedure excludes leveed lands as SWHA regardless of their actual inundation by tide gates, culverts, or flood exceedance, because they are so extensively altered from their natural condition and habitat functions are reduced. Because leveeing is so extensive, this

Table 5 Summary of attribution strategy. See the “Methods” section for descriptions of model and attribution time periods

Factor	Unaltered				Altered			
	Model	Flows	Tides	Topography	Model	Flows	Tides	Topography
Levees	MTP1	ATP1-n	ATP1	Connected	MTP1	ATP1-n	ATP1	Isolated
FNC	MTP1	ATP1-n	ATP1	Connected	MTP3	ATP1-n	ATP3 + 4	Connected
FCRPS	MTP1	ATP3-a	ATP1	Isolated	MTP1	ATP3-o	ATP1	Isolated
FCRPS	MTP1	ATP3-a	ATP1	Connected	MTP1	ATP3-o	ATP1	Connected
Irrigation	MTP1	ATP3-n	ATP1	Connected	MTP1	ATP3-a	ATP1	Connected
Climate change	MTP1	ATP0-n	ATP1	Connected	MTP3	ATP3-n	ATP1	Connected
Total loss	MTP1	ATP1-n	ATP1	Connected	MTP3	ATP3-o	ATP3	Isolated
Subsidence	MTP1	ATP1-n	ATP1	Con. + Subs	MTP1	ATP1-n	ATP1	Connected

a = adjusted; n = naturalized; o = observed; Con. + Subs. = connected + subsidence

departure from KJ2003a,b causes our conclusions to diverge from the earlier study; other reasons emerge below.

The attribution strategy is summarized in Table 5. In addition to the above five attribution factors, the possible effects of subsidence and fill in leveed areas are explored using a sensitivity analysis approach. While subsidence is quite variable over the leveed floodplain, it is plausible that its average value is between 0 and 2 m, based on the available measurements described above. Thus, we examine scenarios that add 0.5 m, 1 m, and 2 m to the LiDAR data in leveed areas to correct for subsidence and subtract 0.5 m in a fourth scenario to represent fill. The underlying assumption is that the historical floodplain was higher (the subsidence scenarios) or lower (the fill scenario) than the present floodplain described by the DTM. The effects of subsidence and fill are then calculated using MTP1 and ATP1 conditions, with connected topography.

Uncertainty

Sources of uncertainty in model results include instrumental errors, uncertainty associated with derived model inputs such as the DTM, flow values, and water-level model parameters. The most uncertain inputs are bathymetry/topography values (collectively, the hypsometry), irrigation withdrawal, and routed flows. The modern DTM used in this study consists of LiDAR and sonar data interpolated onto regular grids. The LiDAR data RMSE is estimated to be approximately 0.05 m for hard-packed surfaces and greater for vegetated surfaces for point clouds prior to processing into a DTM. Uncertainty in modern bathymetry may be as large as 0.1 m, given numerous data sources. Nonetheless, evaluating hypsometry over 1 km increments reduces random errors, as long as there are no systematic errors or strong topographic gradients within a reach (as is generally the case). There is likely a much larger but unquantifiable systematic uncertainty in the historical bathymetry and topography. The

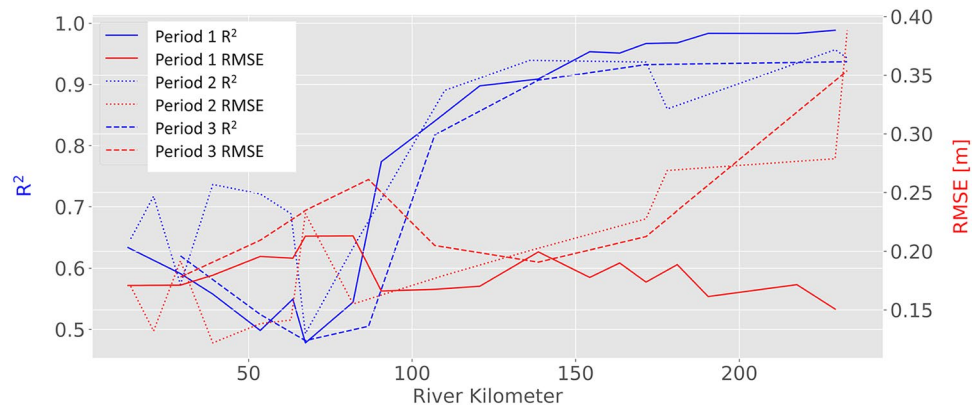
analysis of subsidence, defined above and discussed below, effectively evaluates the effects of hypsometric uncertainty.

HHW was modeled (Eq. 1) via linear regression with flow, tides, and CUI as predictor variables. Model exponents were iteratively optimized by minimizing the root-mean-square error (RMSE) for combinations of model exponent values within exponent ranges identified in Jay et al. (2016). Parameter uncertainty estimates for the water level model were assessed by regressing randomly resampled response and predictor variable data using the optimized exponents to bootstrap the underlying parameter distributions using 10,000 samples of the distributions. Error estimates for each of the attribution scenarios and for total change in SWHA were calculated by propagation of model parameter uncertainty (95th percentile confidence interval) through the calculation of HHW.

There is also systematic uncertainty associated with the attribution strategy, for several reasons: (a) the list of factors evaluated is not exhaustive; (b) the evaluation approach is not unique and a different strategy (e.g., systematically evaluating SWHA in the presence of levees) might yield different answers, and (c) in the real world, factors interact with one another, whereas we largely evaluate only one factor at a time. A sensitivity analysis approach is used to evaluate the effects of perturbations of the attribution strategy on model results. For example, we evaluate the impact of the FCRPS on SWHA assuming both connected and isolated topography, both as a test of uncertainty, and as a guide to management in the real, altered world.

Finally, we will show below that hypsometric uncertainty related to subsidence is the most important factor affecting our SWHA loss estimates and their attribution. In the absence of a conclusive determination of average subsidence, we report results for the zero-subsidence scenario, and use the others to set uncertainty bounds, assuming that 2 m of subsidence is an upper bound on average subsidence. As discussed below, estimates of historical SWHA that account for subsidence are larger than estimates that do not include subsidence.

Fig. 5 R^2 and RMSE for modeling time periods 1, 2, and 3, for stations along the LCRE



Results

Use of Eq. (1) to evaluate SWHA requires that this model accurately reproduces HHW levels for a wide range of conditions. Overall, model performance is good (in terms of R^2 and RMSE) for the tidal stations in Table 4, enabling an evaluation of broad time–space patterns and attribution. The R^2 metric increases in the upstream direction for all three MTPs; it is 0.5–0.7 below rkm100, and greater than 0.85–0.9 farther upstream (Fig. 5). RMSE for MTP1 remains in the range of 0.15–0.22 m. RMSE for MTP2 increases upstream, while MTP3 has a local maximum at rkm-87 due to a known data quality issue, but is otherwise <0.22 m up to rkm-170. The relatively large RMSE near Bonneville Dam in MTP2 and MTP3 is likely due to several factors: (a) a large range of water levels (> 12 m), (b) ongoing bed erosion that changed the water level regime over the time period analyzed (Templeton and Jay 2013), and (c) daily power peaking that strongly influences HHW immediately below the dam (Jay et al. 2015), but is averaged out in the daily flow values used in Eq. 1. Overall, HHW levels during high-flow periods are slightly under-estimated near the dam, but there is little or no SWHA in this reach under high flow conditions. Thus, the effect of model error is negligible.

Long-Term Changes in SWHA

SWHA is highly sensitive to assumed flow conditions and is strongly affected by flow management, so we revisited the scenarios considered by KJ2003a,b by examining all four combinations of naturalized vs. observed flows, and isolated topography vs. connected topography (Fig. 6). For naturalized flows, SWHA predominantly occurs during the historical freshet period (May through July), while under observed flow conditions, SWHA is more spread out through the year, particularly toward the winter and since about 1940. Alteration of the flow cycle from the 1930s to the 1970s was the primary reason for the shift of SWHA away from the freshet, but this shift also reflects warmer

winters and earlier snowpack melt. SWHA for isolated topography for both naturalized and observed flows is substantially lower than for connected topography; the levee system has the largest impact on the loss of SWHA in the system (Fig. 6). However, as noted by KJ2003a,b, there is considerable redundancy in the system, in that both levees and flow regulation/diversion reduce freshet season SWHA, an expected feature of a system engineered in part for flood-control in the LCRE.

Seasonal Variations in Habitat

A seasonal evaluation reveals several SWHA patterns that have changed between ATP1 and ATP3 (Fig. 7A, B). ATP2 results (Table S2 and Fig. S2) more closely resemble ATP3 than ATP1. ATP1 represents the pre-alteration system, ATP2 differs from ATP1 due to construction of the FCRPS, increased irrigation, and deepening of the navigation channel from 9 to 11 m. ATP3 represents the modern system with a 13 m deep navigation channel, a warmer climate, and somewhat altered hydropower management. For the four most seaward reaches, isolated topography has 40–50% less SWHA during both ATP1 and ATP3 than connected topography. Our attribution analysis below will show that differences between ATP1 (Fig. 7A) and ATP 3 (Fig. 7B) are caused by a combination of factors, including changes in hydrology, tides, river slope, and hypsometry. There are also considerable differences in SWHA between reaches, even under connected conditions in both ATP1 and 3 (Fig. 7A, B). The Upper Estuary Reach has the largest amount of SWHA (about 10,000 ha), followed by the Middle Tidal River Reach (~8000 ha), and the Lower Tidal River and Energy Minimum Reaches (both with about ~5000 ha). SWHA values in the Upper Tidal River and The Cascade Reaches are much smaller, regardless of conditions.

Seasonality is strong from the Upper Estuary through the Tidal River, but there is a more complex temporal pattern in ATP3 for most reaches (Fig. 7). The differences between isolated and connected scenarios are particularly strong

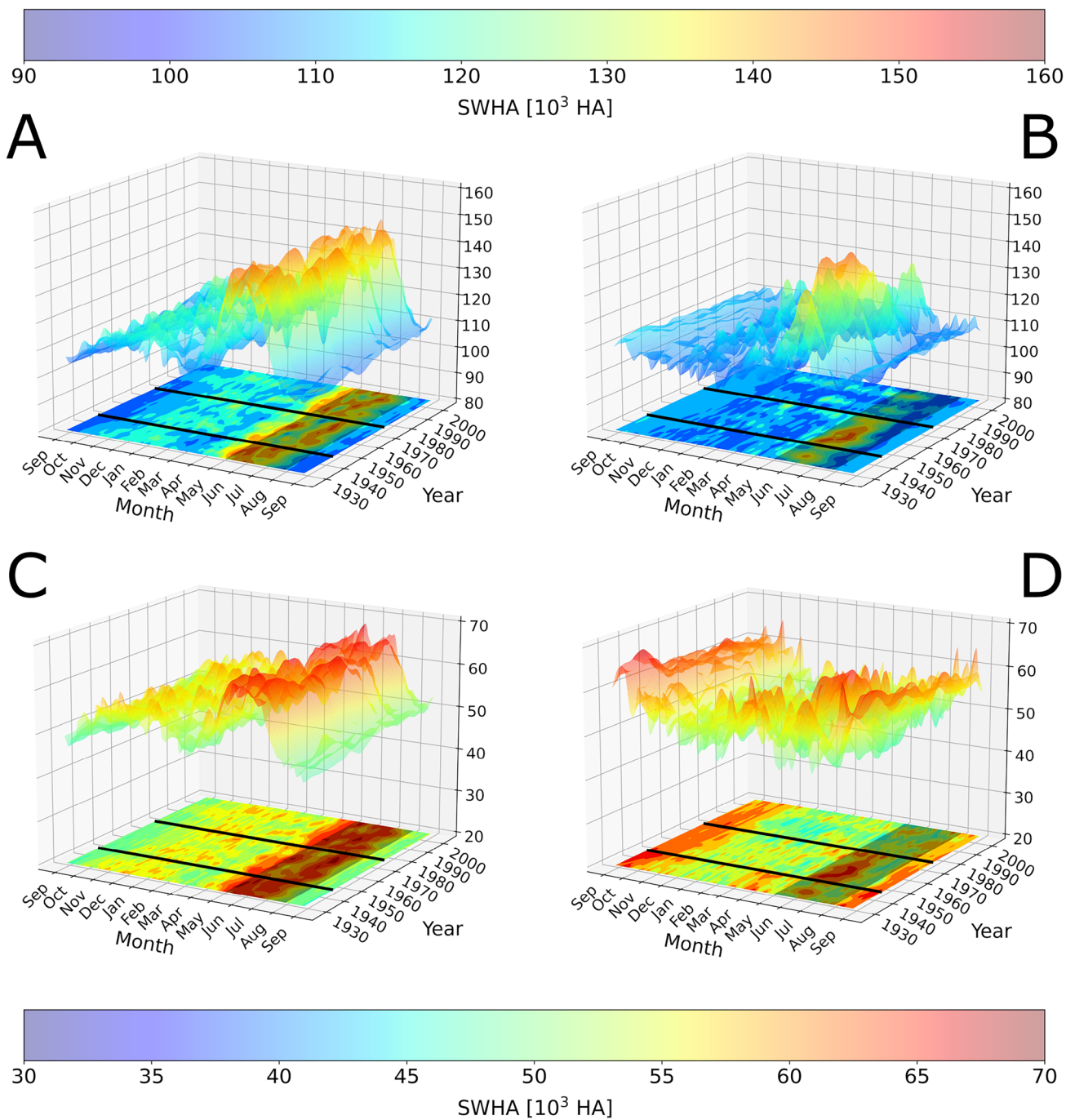


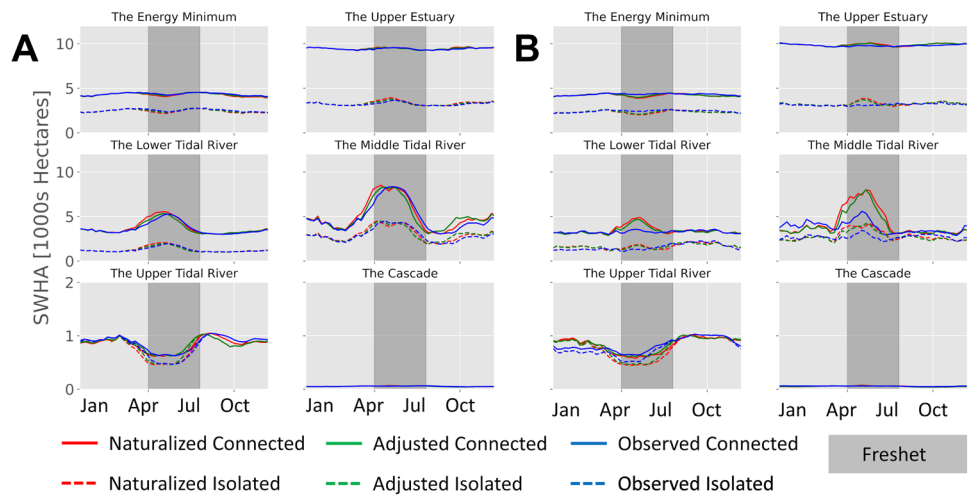
Fig. 6 A 3D perspective of daily SWHA per year (ha/day) for 1928–2004 based on MTP1. Connected topography is depicted in (A) and (B), with isolated topography shown in (C) and (D). Naturalized flows are depicted in (A) and (C) and observed flows in (B) and (D).

The May through July freshet season is shaded in the *x*–*y* plane at the bottom of each sub-panel. Scales for the connected and the isolated topography differ. The boundaries between attribution periods (ATPs 1 to 3) are shown as black lines for 1946 and 1976

during the freshet season (May through July) in the Lower and Middle Tidal River reaches in ATP1. The Upper Estuary Reach exhibits the greatest and seasonally most consistent difference between the isolated and connected scenarios; note the extensive floodplain habitat potential for connected topography (see Fig. 3). Both the Energy Minimum

and the Upper Tidal River reaches show decreased SWHA during the freshet season (see gray areas in Fig. 7A, B). This occurs when high flows inundate large areas of the floodplain to >2-m depth (Fig. 1A), and steep upland topography limits SWHA at the upper edge of the floodplain.

Fig. 7 Daily SWHA averaged annually by reach and month (ha/day) for the six basic scenarios for **A** historical conditions, 1928–1946 (ATP1), and **B** modern conditions, 1976–2004 (ATP3). The freshet season (May through July) is shaded dark gray



The tidal river regions that are strongly forced by river flow exhibit the largest change in water level variability over time; however, the corresponding loss in SWHA depends also on hypsometry, complicating the relationship between altered water level variance and SWHA. Indeed, the strongest changes between ATP1 and ATP3 in SWHA seasonality patterns occurred in the Lower and Middle Tidal River Reaches, not in the upper tidal or Cascade reaches. Specifically, the connected-topography + observed-flow scenario is similar to the other connected scenarios for ATP1, but different in ATP3 (Fig. 7A, B). In ATP1, freshet flows lead to elevated SWHA in the Lower Tidal River, but with a slight dip at peak freshet for all connected scenarios. For the Upper Tidal River, all ATP1 scenarios lose SWHA during the freshet season due to very high water levels, though the losses are larger for the naturalized and adjusted flow

scenarios. In ATP3, the situation changes, and the connected + observed-flow scenario behaves much like the isolated scenarios (Lower Tidal River Reach), or in a unique manner (Middle Tidal River Reach) during ATP3 (Fig. 7). SWHA increases during the freshet, rather than decreasing, in the Lower Tidal River Reach.

Cumulative Impact on Habitat since 1928–1946

We evaluated SWHA for representative high, average, and low flows for historical and modern conditions; the flows were based on inspection of flow records at Bonneville Dam. The net change in aggregate total SWHA for each reach between historical and modern conditions for the chosen events is typically a loss (Table 6), with minor exceptions during low and average flows in the Cascade

Table 6 SWHA for ATP1, ATP2, and ATP3 for representative low, average, and high flow events. Units are 10³ ha

Period	Flow	Energy Minimum	Upper Estuary	Lower Tidal	Middle Tidal	Upper Tidal	Cascade	Total
ATP1	Low	11	10.2	5.6	9.3	0.8	0.0	28.7
	Average	4.8	10.7	3.8	4.3	1.1	0.1	24.7
	High	3.7	8.1	4.1	3.1	0.3	0.1	19.4
ATP2	Low	3.0	3.3	1.2	4.0	1.2	0.0	12.8
	Average	4.7	6.4	2.7	3.7	1.1	0.1	18.8
	High	2.6	4.3	2.6	3.5	0.6	0.1	13.8
ATP3	Low	2.2	3.6	1.0	1.9	1.1	0.0	9.9
	Average	2.6	3.2	1.0	1.6	0.7	0.1	9.2
	High	2.6	3.4	2.1	5.3	0.6	0.1	14.1
ATP3-ATP1	Low	-0.6	-6.6	-4.6	-7.4	0.4	0.0	-18.8
	Average	-2.2	-7.5	-2.7	-2.8	-0.4	0.0	-15.5
	High	-1.1	-4.8	-1.9	2.2	0.3	-0.1	-5.4
ATP3-ATP2	Low	-0.9	0.3	-0.2	-2.1	0.0	0.0	-2.9
	Average	-2.1	-3.2	-1.7	-2.1	-0.4	0.0	-9.6
	High	0.0	-0.9	-0.5	1.7	0.1	0.0	0.3

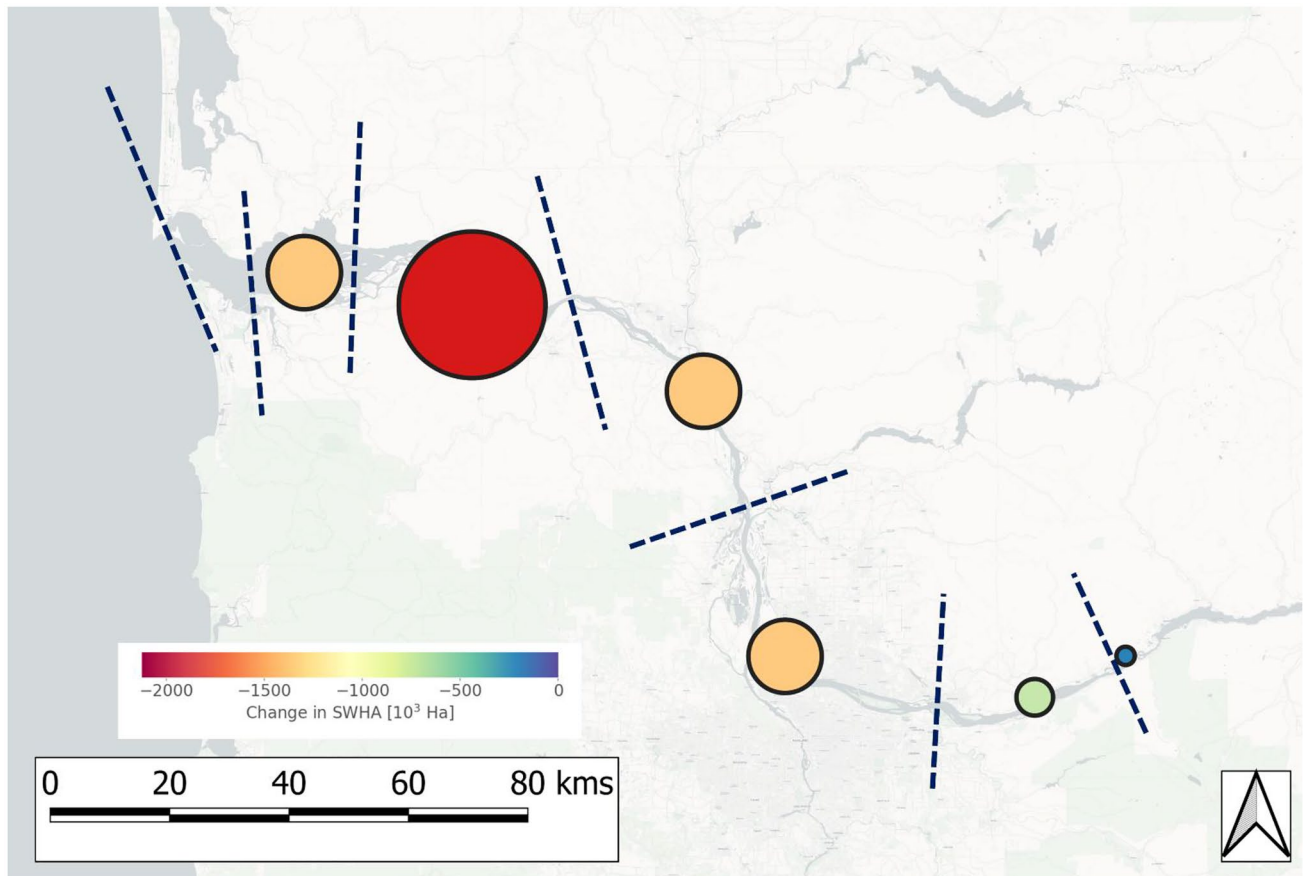


Fig. 8 Total loss of SWHA by reach, including the effects of levees, and changes in flow and tides

Reach, and under high-flow conditions in the Middle Tidal and Upper Tidal Reaches. Essentially, during ATP1, the Cascade, Middle Tidal, and Upper Tidal Reaches are in a state represented by a high-flow condition (Fig. 1A) while in the modern period (ATP3), the middle and upper reaches have shifted to the moderate-flow condition due to changes in river flow through the system (Fig. 1B).

Long-Term Changes in SWHA by Reach

The largest decrease in SWHA occurred in the Upper Estuary—almost three times as much as the Middle Tidal River, the reach with the next largest decrease (Fig. 8). We show below that the levee system plays the dominant role in SWHA loss in the system, except within the Cascade and Upper Tidal River reaches.

For the purpose of conveying the effects of flow changes, model choice, and connectivity, we combined the six reaches into three super-reaches—the Energy Minimum and the Upper Estuary (EM + UE) (1st row, Fig. 9), the Lower and Middle Tidal Rivers (LT + MT) (second row, Fig. 9) and the Upper Tidal River and Cascade (UT + C; third row, Fig. 9). The largest change in SWHA occurs in the middle

super-reach (LT + MT), and is shown by large positive increases (blue coloring) in winter (Nov–March) after 1980, and large decreases (red coloring) during the spring freshet (shaded region). There are small but still significant differences between the two model periods (first and second columns) for all three super-reaches. Overall, there is relatively little change for the UT + C (Fig. 9C, F), although there is a general shift toward more SWHA during the freshet season, regardless of scenario. The increased SWHA for the UT + C is smaller in the presence of levees (Fig. 9I); levees limit SWHA to the lowest elevations, and are frequently covered to more than 2 m in this reach.

Changes in SWHA in the LT + MT are opposite in seasonality to the UT + C. In the modeled absence of levees, there are large net losses in SWHA between ATP1 and ATP3 and a sharp redistribution of SWHA away from the freshet season toward winter and early spring (Fig. 9B, E). This occurs largely due to the flattening of the flow hydrographs in the system from changes in snowmelt and upstream flow regulation. Flow management causes much smaller changes in the presence of levees (Fig. 9H), essentially because the remaining habitat is low and frequently flooded. Similar to the UT + C, SWHA in the EM + UE (first row, Fig. 9) shifts toward freshet season as

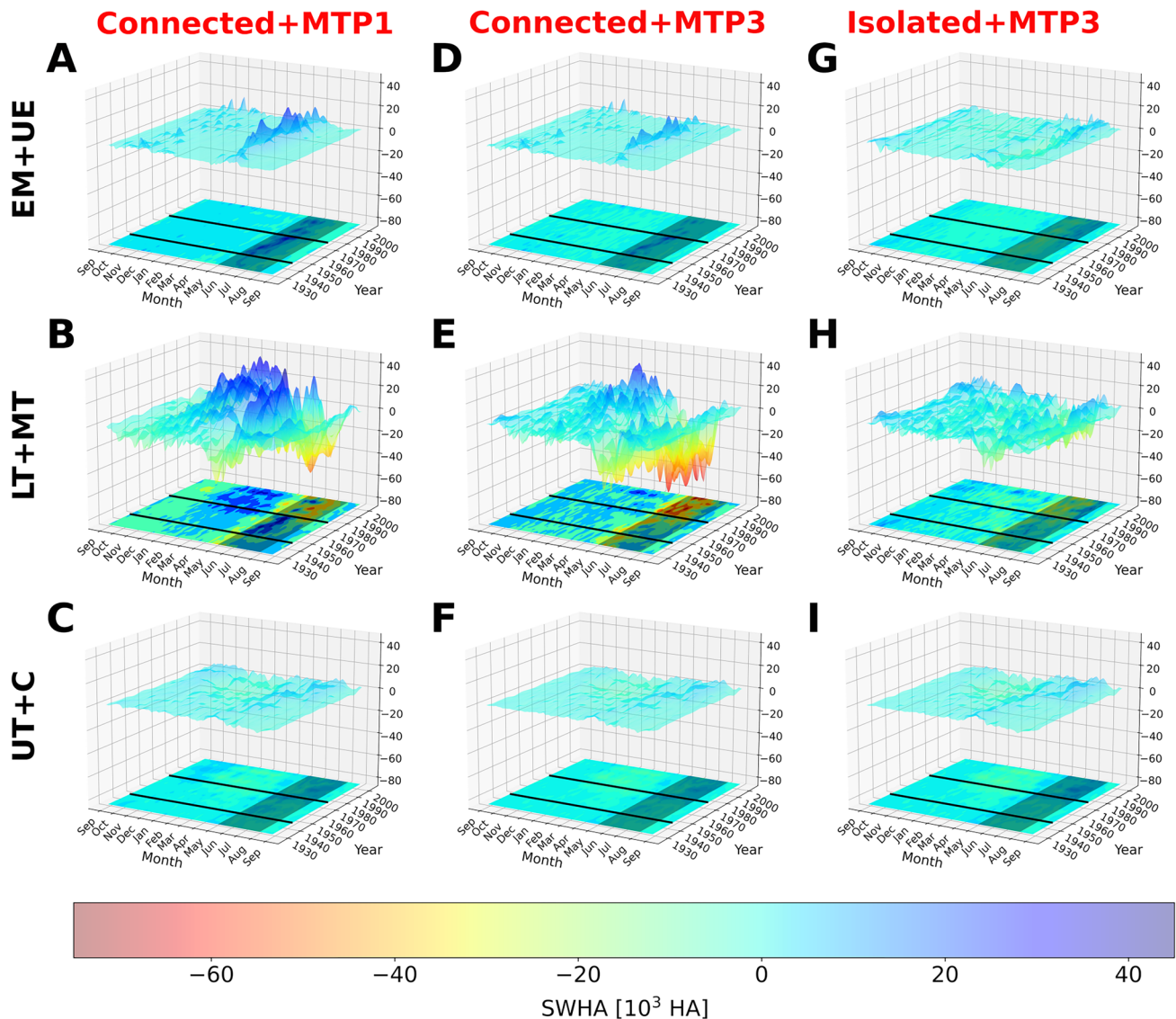


Fig. 9 A 3D perspective of monthly change in SWHA 1928–2004 by decade, using year-day scale data. SWHA change (z-axis) was calculated by differencing SWHA with observed flows from SWHA with naturalized flows using connected topography and MTP1 for (A) the Energy Minimum+Upper Estuary Reaches, (B) the Lower Tidal+Middle Tidal reaches, and (C) the Upper Tidal+Cascade Reaches. SWHA changes were also calculated using connected topography and natural-

ized flows vs. observed flows, with MTP3 for (D) the Energy Minimum and Upper Estuary reaches, (E) the Lower Tidal and Middle Tidal reaches, and (F) the Upper Tidal and Cascade reaches. G–I were calculated as D–F, but with isolated topography. A positive value indicates more SWHA with modified flows. Shading and lines are defined in Fig. 6. The vertical axis depicts the change in SWHA as 10^3 ha

flows are modified, though levees slightly increase the freshet season loss (Fig. 9D vs. Fig. 9G).

A primary observation is that adding levees (Fig. 9G–I) decreases the effects of flow changes (the FCRPS, irrigation and climate change), primarily because there is much less floodplain to inundate. Furthermore, flow management causes, in the absence of levees, a large loss of SWHA in the Lower and Middle Tidal River Reaches, but because levees remove so much potential SWHA, flow-induced changes to SWHA are much smaller in the modern leveed system.

Attribution of Impacts on Habitat

Effectively, the attribution results indicate how levees, flow changes, and changes in tides have altered SWHA (evaluated using modern bathymetry), assuming zero subsidence. The attribution strategy permits analysis of relative contributions to changes in SWHA by the attribution factors in both relative and absolute terms (Fig. 10). Relative changes are percent changes between altered and unaltered conditions for attribution scenarios (Fig. 10A). Absolute changes

Fig. 10 The relative change in SWHA (A) and absolute change with uncertainty error bars (B), by reach, attribution factor, and season (see Table 5). In each attribution group, the leftmost bar group represents the freshet season, the middle bar represents the non-freshet season, and the rightmost bar represents the annual period. The uncertainty bars are based on the 95th percentile uncertainty of the model fit

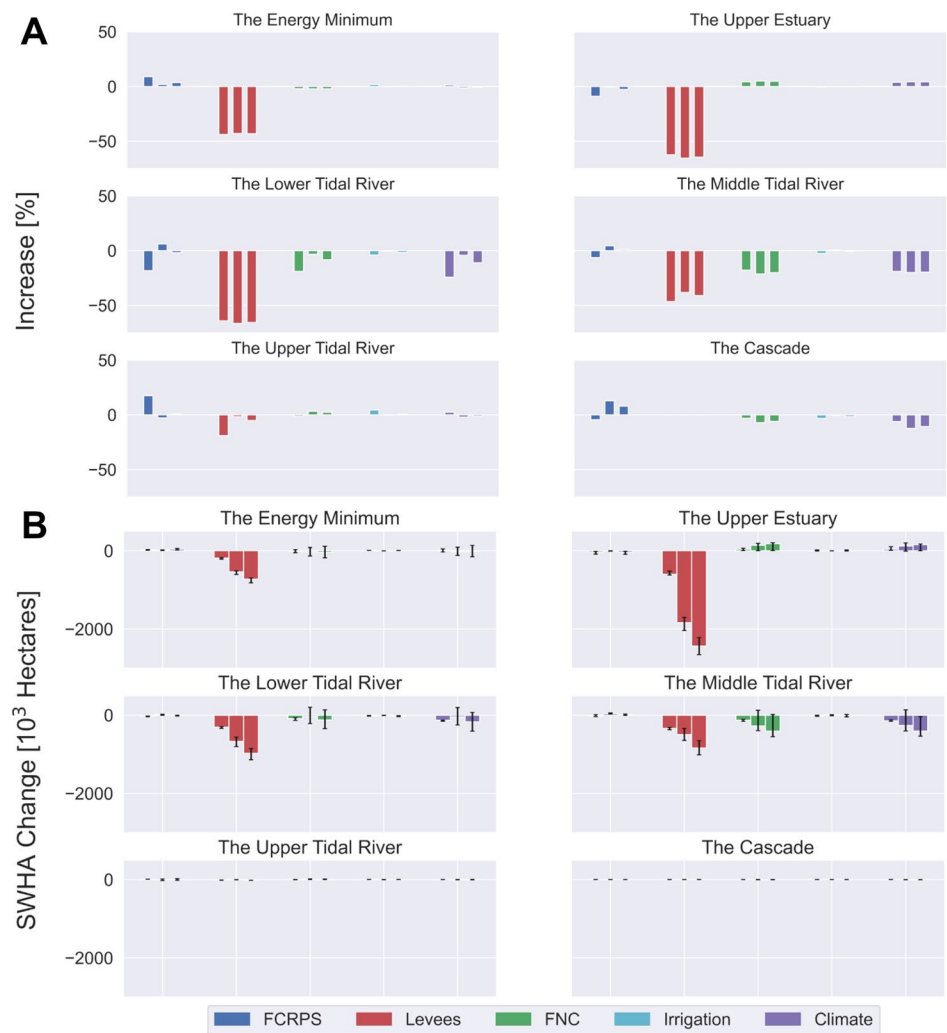


(Fig. 10B) are summed over the season or year. Because the freshet season is only 3 months long, absolute losses may be smaller than for the non-freshet season, even if they are larger in percentage terms. Relative changes (Fig. 10A) are normalized by the total over the period, so that the effect of season length is eliminated. Tables S4A-C provide a detailed breakdown of attribution results by factor and season.

We first discuss attribution based on zero subsidence and uncertainties therein, and then we compare results across subsidence scenarios. Accounting for subsidence alters our results in a systematic way. Considering these differences as systematic uncertainties renders some, but not all, of our estimates more uncertain than indicated by the sensitivity analysis used in Fig. 10.

The levee system has produced the largest relative and absolute impacts on changes in SWHA in the system, with annual average losses of 24×10^5 ha/year in the Upper Estuary Reach and 25×10^5 ha/year collectively between the Energy Minimum, Lower Tidal, and Middle reaches, all reaches that

have been leveed extensively (Fig. 10). Levees have significantly decreased SWHA in all reaches except the Cascade and Upper Tidal River. In percentage terms, losses are relatively uniform across seasons, though cumulative freshet season SWHA losses tend to be smaller than non-freshet losses, because of the shorter duration of the freshet season.

Aside from levees, factors influencing SWHA differ considerably between reaches, and often between seasons (Fig. 10). The FCRPS, irrigation, and climate change all influence water levels and SWHA by modifying the flow cycle; climate change and irrigation both reduce total flow. The FCRPS has a positive effect on SWHA during the freshet season in the Upper Tidal River and Energy Minimum, but a negative effect in the Upper Estuary, Lower and Middle Tidal River, and Cascade reaches. Integrating over all seasons and reaches, the net change due to the FCRPS is essentially zero ($0.02 \pm 3\%$). However, losses during the freshet season most critical to salmonids are extensive, with

losses of up to 15% in the Lower Tidal River and 10% in the Middle Tidal River.

Hydrological shifts caused by climate changes result in generally small increases of SWHA in the more seaward parts of the system but decreases of SWHA farther landward. The net effect is an SWHA loss of $5 \pm 16\%$, which is a symptom of decreased peak flows leading to large decreases in SWHA in the river-dominated reaches. Irrigation has minimal impact on SWHA integrated across all reaches and seasons ($0.4 \pm 1\%$) but causes minor decreases in SWHA in several reaches during the freshet season. Finally, navigation channel development (the FNC) also causes spatially mixed results, with a net loss of about $4 \pm 14\%$ SWHA. The Middle Tidal River stands out for having SWHA losses for all three of the major factors (levees, climate change, and the FNC) in all seasons, while the Lower Tidal River has losses due to all three during freshet season (Fig. 10).

The net influence of the FNC ($4 \pm 14\%$) is the result of interacting factors that partially cancel one another: a long-term reduction in the river surface slope caused by dredging and channelization is counteracted by spatially variable increases in tidal range (see, e.g., Helaire et al. 2019; Talke et al. 2020). Hence, HHW has increased much less than LLW (Helaire et al. 2019; Jay et al. 2011). Also, the increased conveyance capacity of the deeper modern channel moves water more quickly out of the system during high-flow periods, counteracting the loss of storage due to levees (Helaire et al. 2019). In the Upper Estuary, increased tides likely explain increased SWHA (Helaire et al. 2019; Talke et al. 2020), counteracting decreases caused by the FNC farther upstream (Fig. 10). For these reasons, net FNC effects are

limited, though in some reaches the nature of inundation may have shifted to be more tidal than fluvial (Helaire et al. 2020).

The total change in SWHA for the entire system (the sum of the six reaches) is an average annual decrease of 51×10^5 ha/year ($55 \pm 5\%$). Uncertainty in absolute changes in SWHA (Fig. 10B), particularly for attribution scenarios that result in noticeable changes in SWHA (such as levees, in general), fall well within the range of predicted values of SWHA change. For attributions that result in small net changes in SWHA, however, summing SWHA values of opposite sign across reaches can result in an uncertainty level that is high relative to the net change. We will see in the next section, however, that uncertainty regarding subsidence introduces systematic uncertainty larger than this statistical uncertainty.

Effects of Subsidence

The above estimates assume zero subsidence of wetlands behind levees. That is, the elevations used in connected scenarios for all MTPs are derived from modern LiDAR data, though large parts of the diked floodplain have likely subsided. We estimate the sensitivity of our results to subsidence using altered-topography scenarios, using ATP1 flow conditions, and the MTP1 model (Table 5, Fig. 11). SWHA increases as the LiDAR-based bathymetry is raised; the largest increase for historical SWHA in ATP1 occurs by assuming that bathymetry was historically 2 m higher (effectively, this assumes that 2 m of subsidence occurred between ATP1 and ATP3). In the Lower Tidal River, for example, adding 2 m to bathymetry (the 2 m subsidence scenario) results in a more than 125% increase in annual SWHA

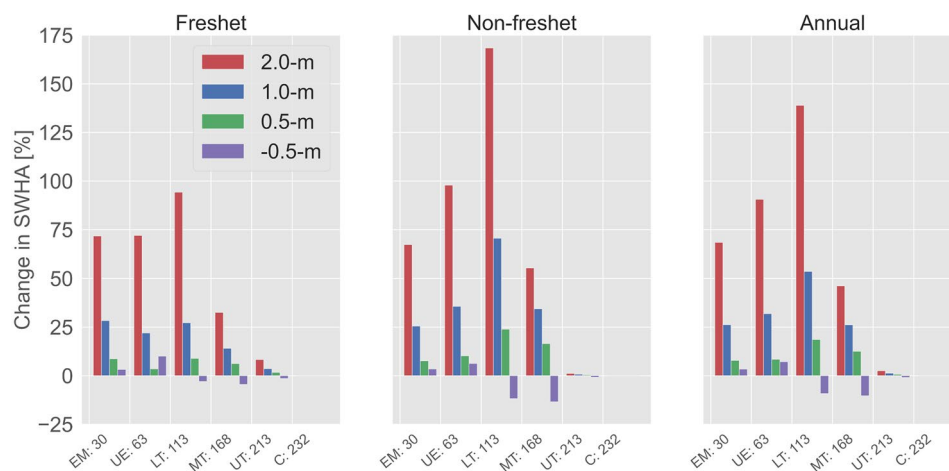


Fig. 11 Percent changes in SWHA in connected conditions, for scenarios of subsidence and infill that may have occurred inside leveed areas (MTP1, ATP1). Corrections of 0.5 m of fill and 0.5 m, 1 m, and 2 m of subsidence are considered for each of the six system reaches. A positive change in SWHA indicates that there is an increase in SWHA between the modern DTM and the modern DTM subsid-

ence scenario. See Table 5 for a summary of attribution strategies. In symbolic form, the following expresses the relationship between SWHA change, the modern DTM, and subsidence: $\Delta_{\text{swha}} = \text{SWHA}_{\text{dtm}} - \text{SWHA}_{\text{dtm+subsidence}}$, where Δ_{swha} is the change in SWHA and $\text{SWHA}_{\text{dtm+subsidence}}$ is the SWHA associated with the modern DTM corrected for subsidence

for isolated topography. More realistic subsidence scenarios of 0.5 to 1 m subsidence result in freshet season and annual changes that do not exceed 30% and 60%, respectively. Interestingly, correcting for fill (assuming ATP1 topography was lower) decreases SWHA in the Middle and Upper Tidal River reaches, likely because water levels are > 2 m during high flow periods over a larger portion of each of these reaches. In contrast, SWHA increases somewhat in the Energy Minimum Reach and the Upper Estuary Reach, because lower topography is more easily inundated, and the 2 m limit is rarely exceeded.

Overall, these results suggest that correcting for subsidence increases estimated ATP1 SWHA, and that the changes would be large in some areas. However, there is no objective means to determine which subsidence or infill/uplift scenario, or combination thereof, is most likely, so we assume zero subsidence for the attribution analysis (Fig. 10).

Model Sensitivity

We next evaluate the significance of our results with regards to systematic and random errors. Model sensitivity was evaluated against flows, irrigation withdrawals, coastal upwelling, and tides (as great diurnal range or GDR), in addition to the above sensitivity analyses of subsidence/infill. Flows, CUI, and GDR were varied by $\pm 10\%$ and irrigation withdrawals were varied by $\pm 50\%$; all were applied to total change in SWHA (ATP3-ATP1). These are relatively large fluctuations in the parameters relative to expected error. It is unlikely that, averaged over any extended period, the major forcing variables (flows and GDR) deviate from the reported measured values by $\pm 10\%$, and these are magnitudes more representative of random deviations. Irrigation withdrawal is, in contrast, poorly known, and substantial systematic errors are possible. Overall, the calculation is intentionally conservative.

Model sensitivity is larger for upstream reaches than downstream reaches, particularly for flow-based variation (Table 7). Variation in coastal upwelling produces small changes in SWHA compared to either flow or GDR. Variation in GDR produces relatively larger variations in SWHA in the upstream reaches. The larger variation in SWHA farther upstream can be attributed to a generally stronger response (per unit change in forcing) in water levels in the Tidal River and Cascade for both flows and tides. Uncertainty in coastal upwelling and processes has a relatively small impact on SWHA because this study focuses on river reaches upstream of salinity intrusion so coastal influences other than tides are generally small. Note that the sign of the SWHA response to a positive change to GDR and flow varies with reach. Whether an increase in flow or tidal range increases SWHA depends critically on the bathymetry and hypsometry of the reach, because increasing inundation can either increase or decrease SWHA (see Fig. 1). If the

Table 7 Relative change in SWHA due to a $\pm 10\%$ perturbation in the predictor variable

Reach	Predictor variable	Effect on estimated change in mean annual SWHA [%]
Energy Minimum	Flow	+1.5/−1.8
	CUI	−0.0/−0.0
	GDR	−0.8/−2.3
	Irrigation	−3.3/+2.5
Upper Estuary	Flow	−0.1/−0.2
	CUI	−0.0/+0.0
	GDR	+1.0/−4.8
	Irrigation	−0.0/−0.3
Lower Tidal	Flow	+6.1/−6.7
	CUI	+0.2/−0.2
	GDR	+18.5/−24.2
	Irrigation	+1.8/−1.9
Middle Tidal	Flow	−3.8/+3.9
	CUI	+0.2/−0.3
	GDR	+19.1/−14.9
	Irrigation	+1.6/−1.6
Upper Tidal	Flow	+73.6/−86.0
	CUI	+0.5/−0.5
	GDR	+29.0/−25.8
	Irrigation	−8.2/+4.8
Cascade	Flow	−26.5/+10.5
	CUI	−1.0/+0.9
	GDR	−2.8/+2.6
	Irrigation	−18.4/+18.5
Total	Flow	+0.9/−1.2
	CUI	+0.1/−0.1
	GDR	+7.3/−9.8
	Irrigation	+0.1/−0.4

floodplain cross-sectional topography varies linearly within a reach from channel to shore, SWHA will remain constant as a function of elevation. For many reaches, SWHA remains approximately constant (relative to its average) for many elevation bands, leading to only modest sensitivity to FNC and FCRPS changes (Fig. 3). Because of differences in response between reaches, the system sensitivity is less than reach sensitivity. With the exception of varying GDR, the net changes are close to or less than 1%, and GDR produces variations of less than 10% for the entire system.

Another potential source of model uncertainty lies with the attribution methodology used. Kukulka and Jay (2003b), for example, assume that leveed areas are isolated when water surface elevations fall below levee crest elevations, but become SWHA at water levels above the levee crest elevation. We assume that leveed areas are never SWHA,

even when flooded. The effects of this methodological choice vary throughout the system, but they are large. We see an increase in the loss of SWHA of 112% (17×10^3 to 35×10^3 ha/year) in the Upper Estuary Reach and a 247% increase (9×10^3 ha/year of loss to 13×10^3 ha/year of gain) in the gain of SWHA in the Middle Tidal Reach, respectively, when FCRPS effects are evaluated with the levees in place (Table S8 in the Supplement). This further emphasizes the importance of the levee system on SWHA.

Hypsometric Uncertainty

We used the differences across the subsidence scenarios as a measure of systematic hypsometric uncertainty in SWHA loss (i.e., ATP1 minus ATP3 SWHA for connected conditions). Five scenarios of assumed average change in the elevation of presently leveed areas were evaluated: no fill/subsidence (zero subsidence), 0.5 m fill, and 0.5 m, 1 m, and 2 m subsidence (Table 8). Specifically, the 0.5 m subsidence scenario assumes that leveed areas subsided 0.5 m since 1928 due to leveeing. Accordingly, evaluating their connected SWHA during ATP1 requires adding 0.5 m to their elevation, as represented by modern LiDAR. Given the LCRE subsidence values discussed above, we consider that the 0, 0.5, and 1 m subsidence scenarios encompass a realistic range; the two extreme scenarios (0.5 m fill and 2 m subsidence) are presented to allow understanding trends with respect to hypsometric change. The zero-subsidence scenario is the one that has been discussed previously.

We then evaluate the total uncertainty of our SWHA loss estimates as follows. Each upper and lower bound is considered separately, and the larger of the values from the model uncertainty analysis and subsidence scenarios is considered to be controlling, with subsidence uncertainty controlling the uncertainty sign. On this basis, our overall attribution analysis estimates of SWHA loss are:

- Total: $55 \pm 5\%$; the model uncertainty and hypsometric uncertainties are the same.
- Levees: $54 \pm_{14}^5\%$; the upper limit is from the model uncertainty, the lower from comparison of the 0 m and 1 m subsidence scenarios.
- FNC (navigation)s: $4 \pm_6^{14}\%$; lower limit from the model uncertainty analysis, the upper from comparison of the 0 m and 1 m subsidence scenarios.
- FCRPS (reservoir system): $0.02 \pm_1^3\%$; as for the FNC.
- Climate-induced hydrologic change: $5 \pm_5^{16}\%$; as for the FNC.
- Irrigation depletion: $0.4 \pm 1\%$; the model and hypsometric uncertainties are similar.

The system-wide, annual average SWHA losses, and uncertainties therein, do not explain all variability; seasonal variability changes depending on scenario and

Table 8 Annual average SWHA losses (ATP3-AT1) by factor and season for the five subsidence scenarios

Season	Freshet	Non-freshet	Annual
0 m subsidence			
Levees	-54.40%	-53.34%	-53.55%
FNC	-6.12%	-3.59%	-4.10%
FCRPS	-4.95%	1.19%	-0.02%
Irrigation	0.09%	-0.47%	-0.36%
Climate	-3.22%	-4.99%	-4.64%
Sum of factors ^a	-68.60%	-61.20%	-62.67%
Total change ^b	-62.86%	-52.87%	-54.88%
Infill 0.5 m (DTM - 0.5 m)			
Levees	-52.60%	-54.56%	-54.18%
FNC	-4.39%	-10.11%	-9.00%
FCRPS	-0.40%	1.44%	1.10%
Irrigation	1.63%	-0.27%	0.08%
Climate	-0.13%	-10.60%	-8.68%
Sum of factors	-55.89%	-74.10%	-70.68%
Total change	-63.68%	-61.45%	-61.88%
Subsidence 0.5 m (DTM + 0.5 m)			
Levees	-52.87%	-47.97%	-49.03%
FNC	-10.29%	-16.31%	-15.01%
FCRPS	-10.59%	1.07%	-1.38%
Irrigation	-1.77%	-0.79%	-1.00%
Climate	-8.75%	-19.79%	-17.45%
Sum of factors	-84.27%	-83.79%	-83.87%
Total change	-63.89%	-55.86%	-57.60%
Subsidence 1 m (DTM + 1 m)			
Levees	-47.31%	-37.20%	-39.52%
FNC	-14.79%	-18.71%	-17.82%
FCRPS	-15.62%	0.99%	-2.72%
Irrigation	-3.47%	-1.00%	-1.56%
Climate	-14.51%	-23.02%	-21.08%
Sum of factors	-95.70%	-78.94%	-82.70%
Total change	-59.63%	-46.72%	-49.68%
Subsidence 2 m (DTM + 2 m)			
Levees	-30.59%	-15.84%	-19.27%
FNC	-20.23%	-21.42%	-21.14%
FCRPS	-17.33%	1.15%	-3.05%
Irrigation	-4.70%	-1.05%	-1.91%
Climate	-20.40%	-25.13%	-24.02%
Sum of factors	-93.25%	-62.29%	-69.39%
Total change	-46.82%	-28.60%	-32.84%

^aThe sum of factors represents the sum of the levee, FNC, FCRPS, irrigation, and climate attribution factors

^bThe total change represents the difference between the base condition and the Modern system with observed flows and isolated topography

factor (Table S6). Freshet season SWHA loss ranges narrowly from 60 to 63% over the subsidence scenarios, but FCRPS total losses range from ~5 to 16%, and FNC and climate total losses also reach ~15% in the 1 m subsidence

scenario. Spatially, the zero-subsidence scenario suggests SWHA loss of 59–76% in the Upper Estuary and lower Tidal River, depending on season; both reaches have large amounts of SWHA. Energy Minimum seasonal losses decrease from 41–44% (zero-subsidence) to 26–29% (1 m subsidence) for the 1 m subsidence scenario.

It is useful also to understand how the impacts of various attribution factors vary as hypsometry is changed (Table 8). As subsidence increases, factors that have reduced mean or peak spring flows (the FCRPS, irrigation, and climate change) produce a greater impact during the freshet season and annually. Reduced flows cause lower water levels, so that less SWHA can be inundated as assumed floodplain elevations rise. Non-freshet season impacts of these factors are mixed, because of the transfer of flow into the winter season in recent decades. Also, the FNC reduces along-channel mean water slope in all seasons, and this factor seems to be more important than increased tidal amplitudes; thus, the FNC is more impactful in all seasons as subsidence correction increases. On the other hand, increasing the subsidence correction reduces the estimated leveeing impacts in all seasons, because the inundated area itself becomes smaller as assumed historical floodplain elevation is raised, and the floodplain cannot be inundated regardless of levees.

Finally, Table 8 shows that the sum of the individual factors is larger, on an annual average basis, than the total loss, because factors overlap and interact. This difference increases from about 8 to 33% as the subsidence correction increases from 0 to 1 m. For the zero-subsidence scenario on which our analysis is primarily based, the sum of factors is 63%, compared to the total loss of 55%; we regard this as support of the single-factor analysis approach employed in this study.

Discussion and Conclusions

Changes in the processes and configuration of the LCRE greatly reduced SWHA in the system 1928–2004. The largest contributing factor to both the absolute and the relative percent changes is the presence of levees that isolate the floodplain from the Columbia River (Fig. 10). By reducing available area for shallow-water inundation, levees decrease the relative impact of the hydropower system on SWHA. In the Upper Estuary and the Lower Tidal River, SWHA has decreased by over 50% for all times of the year for the zero-subsidence scenario (freshet, non-freshet, and annual—Fig. 10). Seasonality is important to habitat function and, with few small exceptions, all attribution factors (levees, land subsidence and infill, the hydropower system (FCRPS), the navigation channel (FNC), irrigation withdrawals, and climate change) have contributed to decreases in freshet

season SWHA. Important exceptions are the FCRPS in the Energy Minimum and Upper Tidal River, the FNC in the Upper Estuary, and the FNC and Irrigation in the Upper Tidal River (Fig. 10). These freshet season losses are particularly important, because this is the season when SWHA use by juvenile salmonids is greatest.

Both the absolute and relative contributions of attribution factors to loss of SWHA in the system have implications for future management and restoration decisions. The dominant influence of the levee system on SWHA loss provides a basis for prioritizing reconnection of floodplains via levee breaching, and Columbia Estuary Ecosystem Restoration Program (CEERP) has in fact prioritized this method 2004–present (Littles et al. 2022). Although FCRPS impacts on SWHA are smaller than those of levees, relative losses are measurable in four of six reaches during the freshet season (Fig. 10A), when climate change, irrigation diversion and hydropower management work in concert to decrease flows. However, FCRPS impacts are spatially variable, and levees have isolated most higher floodplain elevations, leaving only un-leveed portions of the floodplain near the thalweg. This means that any proposed changes to the flow regime in a leveed system need to be carefully analyzed. Conversely, restoration planning needs to consider present and likely future inundation patterns. For instance, past climate change effects on the hydrologic cycle produce relatively large impacts on SWHA in the Middle Tidal River (Fig. 10); future analyses of restoration impacts on SWHA in the Middle Tidal River should therefore consider alterations to the hydrologic cycle from future climate change. In addition to the stressors considered here, other recent work suggests that co-seismic subsidence caused by a magnitude 9+ Cascadia Subduction Zone earthquake would alter or eliminate nearly all wetland habitats in the lower estuary, until the system readjusted (Brand et al. 2023).

The largest absolute decreases in SWHA attributable to levees occur in the Upper Estuary and Lower and Middle Tidal Rivers, though substantial losses also occur in the Energy Minimum. (Fig. 10B). The most noticeable increase in SWHA caused by navigational development (the FNC) is seen in the Upper Estuary, while climate change impacts are strongest in the Lower and Middle Tidal River and Cascade Reaches (Fig. 10). For all factors and periods, a complex interplay between flows, tides, coastal processes, and changing hypsometry determines SWHA in the system, a fact dictated by the nonlinear nature of Eq. 1. Also, the 2 m upper limit on SWHA and the non-monotonic nature of the hypsometric curves (Fig. 3) sometimes affect the SWHA response to flow in a counter-intuitive way, as increasing water levels do not always translate into more SWHA.

For representative flow conditions—low, medium, and high—patterns in the total loss of SWHA across reaches highlight the importance of the unique physical

characteristics of each reach (Table 6). The lower three Reaches analyzed (the Energy Minimum through Lower Tidal River) all see decreases of 20% or more in SWHA for all flow conditions, whereas the more landward reaches are more variable in their responses; for example, decreased freshet flows have increased SWHA in the Middle and Upper Tidal River during high flow conditions (Table 6). With a general flattening of the flow hydrograph from the earliest time period (ATP1, starting in 1928) to ATP3, modern high flows behave more like historical average flows; this can increase or decrease SWHA, but net changes due to the FCRPS are small compared to those caused by the levee system and development of the floodplain through levee construction and land conversion.

Accounting for subsidence and infill of leveed areas alters estimated ATP1 SWHA for varying levels of land subsidence (Fig. 11) and introduces systematic uncertainties into results that are larger than statistical uncertainties for some factors and seasons. Thus, correcting for 0.5–1 m of subsidence since 1928 results in increased estimates of SWHA loss, although the degree varies widely between reaches. While the degree of subsidence in the system has not been ascertained, the relationships between changing land surface elevation and SWHA documented here may help provide guidelines for target elevations in future floodplain habitat restoration.

Most of the estimated reduction in SWHA in the LCRE is due to the levee system. Independent of the levee system (Fig. 10), however, there is considerable spatial and temporal variation of SWHA in the system (Fig. 9). For the Upper Estuary and Lower and Middle Tidal River reaches combined, SWHA availability has shifted away from the freshet period in ATP3 (Fig. 10). This shift is due to alteration of the flow regime, caused by the FCRPS (flood control and power generation), irrigation, and climate change. The timing of seasonally reduced SWHA in these reaches coincides with relatively high historical and contemporary abundances of Chinook salmon fry in the LCRE—and in the later months of the freshet, fingerlings (Bottom et al. 2005; Burke 2004; Dawley et al. 1985, 1986; Roegner et al. 2016; Sather et al. 2016).

The sensitivity of upstream reaches to flow scenarios occurs because water levels respond to river flow to a greater degree farther from the Pacific, with correspondingly greater variations in water level (Borde et al. 2020; Jay et al. 2015). Changing hydrology (the FCRPS, irrigation, and climate change) has caused generally small (and sometimes positive) SWHA changes between ATP1 and ATP3 in the estuary reaches analyzed (Table S6; see also Table S7). These are related to both an altered annual hydrograph and a decrease in flow variance. Another factor not considered here is the impact of altered tidal monthly variations in water level that result from the interactions of changing tides and altered hydrology. Finally, we are unable to estimate the effects of

changes in the flow regime on hypsometry due to altered sedimentation patterns including reduced sediment supply (Naik and Jay 2011b) and ensuing hypsometric effects (e.g., Templeton and Jay 2013; Jay and Simenstad 1996).

Key takeaways from the present study include the following:

- SWHA in the LCRE has decreased by $55 \pm 5\%$, or 51×10^5 ha/year. The primary factor driving this decrease on an annual basis is isolation of the floodplain by leveeing and development ($54 \pm 5\%$). In aggregate, the FNC reduces SWHA by $4 \pm 14\%$, climate change by $5 \pm 16\%$, and irrigation withdrawal by $0.4 \pm 1\%$. Uncertainty limits on these estimates consider both model-parameter and hypsometric sensitivity.
- The hydropower system (FCRPS) has only a small net effect on annual average SWHA ($0.02 \pm 1\%$) for the system as a whole. However, its effects are spatially and temporally variable, and as levees are breached for restoration, the relative importance of FCRPS impacts will increase.
- In the modern system with extensive levees, floodplain areas that remain are low and therefore subject to inundation > 2.0 m by very high flows, exceeding criteria for SWHA. Present, reduced freshet flows accordingly produce some gains in habitat in the leveed system in some reaches.
- When high abundances of Chinook salmon fry and fingerlings are in the LCRE during the freshet season, SWHA in reaches from the Energy Minimum to the Middle Tidal River (rkm21–196) has greatly decreased. These reaches have been the focus of much floodplain wetland restoration by CEERP, so changes and potential improvements in SWHA warrant further analysis.
- Floodplain isolation by levees reduces SWHA throughout the system and in all seasons, whereas the other attribution factors have spatially and seasonally variable effects. Seasonal variation for the FNC and climate change are more pronounced than other attributes for the Upper Estuary and the Lower Tidal and Middle Tidal River.
- Failure to account for subsidence, i.e., using modern floodplain elevations as an estimate of historical elevations, increases estimated historical SWHA, and the magnitude of over-estimation increases with subsidence.
- Alteration of the flow cycle from the 1930s to the 1970s was the primary reason for the shift of SWHA from freshet season to the rest of the year, but this shift also reflects warmer winters, earlier snowpack melt, and levees reduce freshet season SWHA.
- SWHA is a measure of habitat area, not quality, and this study did not measure whether the lower elevation spring SWHA now available has the same quality as the higher elevation SWHA historically available, when spring flows were much higher and dikes absent.

The results of this study diverge considerably from those of KJ2003a,b, in that the FCRPS is found here to be a rather small factor in SWHA reduction on an annual average basis, whereas it was a much larger factor in KJ2003a,b. This altered conclusion is mostly caused by a change in the definition of SWHA. KJ2003a,b included leveed areas in the calculation of FCRPS effects, whenever water levels exceeded levee crest elevations. Here, we only attribute FCRPS effects to regions with currently viable habitat, and attribute loss behind levees to the construction of this infrastructure. The assumed hypsometry constitutes another major difference between the two studies. The topography used by KJ2003a,b represented a system with a lesser degree of subsidence, was much less detailed, and had higher uncertainty levels reflecting standards at that time. Without recreating their analysis, we are unable to quantify the differences in results due to hypsometry, but our analysis of subsidence scenarios suggests that hypsometric uncertainty strongly impacts estimates of SWHA loss. Finally, KJ2003a,b studied only a reach within the Upper Estuary, a reach for which our results also show freshet season losses of SWHA due to FCRPS operation.

Other methodological factors also constrain or influence our conclusions. A primary factor is the definitional requirement per Bottom et al. (2005) that the water level of SWHA not exceed 2 m; different depth limits may change results. While the supply of spatially and temporally comprehensive water level datasets in the system is a limitation, this is true of any statistical or numerical approach used in a study on a centennial basis and spanning hundreds of kilometers. The primary advantage of the statistical approach used in this study over a numerical approach is that it can be applied over very large areas and time periods with minimal computational expense. This enables multiple scenarios and an assessment of uncertainty that would be difficult to carry out in a numerical model. Finally, the attribution approach considers the five major attribution factors individually; however, FCRPS effects are evaluated with both isolated and connected topography, to understand the interactions of the diking and the FCRPS. The remaining attribution factors are also not completely independent; for example, some FCRPS dams were constructed as irrigation projects, with hydropower and flood control as secondary objectives.

The methodology used here should be broadly applicable to evaluation of long-term changes in systems used by migrating salmonids; i.e., along the West Coast of North America and beyond (Bidlack et al. 2021; Bond et al. 2018; Buijse et al. 2002; Opperman et al. 2010). Countless anthropogenically altered systems have been marked by secular shifts in floodplain connectivity, river hydrographs, tides, and river slope. Examples include the Hudson River (Ralston et al. 2019) and Saint Johns River (Talke et al. 2021). Although hypsometric effects and hydrodynamic change are individual to each system, our

method is potentially useful elsewhere where historical water level datasets are available or recoverable for use in mapping changes in SWHA.

Supplementary Information The online version contains supplementary material available at <https://doi.org/10.1007/s12237-023-01229-3>.

Acknowledgements This study was supported by the Bonneville Power Administration through project 2002-077-00 led by Pacific Northwest National Laboratory (PNNL). We thank graphic artist Nathan Johnson for preparing Fig. 1, and Amy B. Borde, Columbia Land Trust, for technical review of Fig. 1 and updates to the geospatial data for levees based on her field observations. We thank Shon A. Zimmerman, PNNL, for sharing river kilometer delineations. Water level and flow data used in this study are archived at PDXScholar: <https://doi.org/10.15760/cee-data.08>. HHW level model coefficients are listed in the Supplementary Material.

Open Access This article is licensed under a Creative Commons Attribution 4.0 International License, which permits use, sharing, adaptation, distribution and reproduction in any medium or format, as long as you give appropriate credit to the original author(s) and the source, provide a link to the Creative Commons licence, and indicate if changes were made. The images or other third party material in this article are included in the article's Creative Commons licence, unless indicated otherwise in a credit line to the material. If material is not included in the article's Creative Commons licence and your intended use is not permitted by statutory regulation or exceeds the permitted use, you will need to obtain permission directly from the copyright holder. To view a copy of this licence, visit <http://creativecommons.org/licenses/by/4.0/>.

References

- Al-bahadily, A. 2020. Long term changes to the Lower Columbia River Estuary (LCRE) hydrodynamics and salinity patterns. PhD thesis. Portland State University, Portland, OR. <https://doi.org/10.15760/etd.7357>
- Bakun, A. 1973. Coastal upwelling indices, West Coast of North America, 1946-71. U.S. Dep. Commer. NOAA Tech. Rep., NMFS SSRF-671. 103.
- Bidlack, A.L., S. Bisbing, B. Buma, H. Diefenderfer, J. Fellman, W. Floyd, and I. Giesbrecht. 2021. Climate-mediated changes to linked terrestrial and marine ecosystems across the Northeast Pacific Coastal Temperate Rainforest Margin. *BioScience*. <https://doi.org/10.1093/biosci/biaa171>
- Blumm, M.C. 2002. *Sacrificing the salmon: A legal history of the decline of Columbia basin salmon*. BookWorld Publishers.
- Bond, M.H., T.G. Nodine, T.J. Beechie, and R.W. Zabel. 2018. Estimating the benefits of widespread floodplain reconnection for Columbia River Chinook salmon. *Canadian Journal of Fisheries and Aquatic Sciences* 76: 1212–1226.
- Borde, A.B., H.L. Diefenderfer, S.A. Zimmerman, V.I. Cullinan, and R.M. Thom. 2020. Ecohydrology of wetland plant communities along an estuarine to tidal river gradient. *Ecosphere* 11(9). <https://doi.org/10.1002/ecs2.v11.9>
- Bottom, D.L., C.A. Simenstad, J. Burke, A.M. Baptista, D.A. Jay, K.K. Jone, E. Casillas, and M.H. Schiewe. 2005. Salmon at river's end: the role of the estuary in the decline and recovery of Columbia River salmon. NOAA Technical Memorandum NMFS-NWFSC-68.
- Bottom, D.L., A. Baptista, J. Burke, L. Campbell, E. Casillas, S. Hinton, D.A. Jay, M.A. Lott, G. McCabe, R. McNatt, M. Ramirez, G.C. Roegner, C.A. Simenstad, S. Spilseth, L. Stamatiou, D. Teel, and J.E. Zamon. 2011. Estuarine habitat and juvenile salmon: Current

- and historical linkages in the Lower Columbia River and Estuary. US Army Corps of Engineers.
- Brand, M.W., H.L. Diefenderfer, J.E. O'Connor, A.B. Borde, A. Jay, A. Al-Bahadily et al. 2023. Impacts of a Cascadia subduction zone earthquake on water levels and wetlands of the lower Columbia River and estuary. *Geophysical Research Letters* 50: e2023GL103017. <https://doi.org/10.1029/2023GL103017>
- Buijse, A.D., H. Coops, M. Staras, L.H. Jans, G.J. Van Geest, R.E. Grift, B.W. Ibelings, W. Oosterberg, and F.C. Roozen. 2002. Restoration strategies for river floodplains along large lowland rivers in Europe. *Freshwater Biology* 47 (4): 889–907.
- Bunn, S.E., and A.H. Arthington. 2002. Basic principles and ecological consequences of altered flow regimes for aquatic biodiversity. *Environmental Management* 30: 492–507.
- Burgette, R.J., R.J. Weldon II., and D.A. Schmidt. 2009. Interseismic uplift rates for western Oregon and along-strike variation in locking on the Cascadia Subduction Zone. *Journal of Geophysical Research* 114: B01408.
- Burke, J.L., 2004. Life histories of juvenile Chinook salmon in the Columbia River Estuary, 1916 to the present. Master of Arts Thesis, Oregon State University, Corvallis, OR.
- Callaway, J.C., A.B. Borde, H.L. Diefenderfer, V.T. Parker, J.M. Rybczyk, and R.M. Thom. 2012. Pacific Coast tidal wetlands. *Wetland habitats of North America: ecology and conservation concerns*, 103–116. Berkeley, CA: University of California Press.
- Cannon, C.M., 2015. Landforms along the Lower Columbia River and the Influence of Humans. Portland State University, MS thesis.
- Dawley, E. M., R.D. Ledgerwood, and A.L. Jensen. 1985. Beach and purse seine sampling of juvenile salmonids in the Columbia River estuary and ocean plume, 1977–1983; Volume I: procedures, sampling effort, and catch data, Vol. II: Data on marked fish recoveries. NOAA Technical Memorandum. NMFS F/NWC-75. 334 pp.
- Dawley, E. M., R. D. Ledgerwood, T.H. Blahm, C.W. Sims, J.T. Durkin, R.A. Kirn, G.E. Monan, and F. J. Osslander, 1986. Migrational characteristics, biological observations, and relative survival of juvenile salmonids entering the Columbia River estuary, 1966–1983. Coastal Zone and Estuarine Studies Division, NMFS-NOAA and Bonneville Power Administration. Contract No. DE-AI79–84-BP39652, Project No. 81–102. 256 pp.
- Diefenderfer, H.L., A.B. Borde, and V.I. Cullinan. 2021. Floodplain wetland channel planform, cross-sectional morphology, and sediment characteristics along an estuarine to tidal river gradient. *Journal of Geophysical Research: Earth Surface* 126: e2019JF005391.
- Diefenderfer, H.L., A.M. Coleman, A.B. Borde, and I.A. Sinks. 2008. Hydraulic geometry and microtopography of tidal freshwater forested wetlands and implications for restoration, Columbia River, USA. *Ecohydrology & Hydrobiology* 8 (2–4): 339–361.
- Diefenderfer, H.L., G.E. Johnson, R.M. Thom, K.E. Buenau, L.A. Weitkamp, C.M. Woodley, A.B. Borde, and R.K. Kropp. 2016. Evidence-based evaluation of the cumulative effects of ecosystem restoration. *Ecosphere* 7 (3): e01242.
- Diefenderfer, H.L., I.A. Sinks, S.A. Zimmerman, V.I. Cullinan, and A.B. Borde. 2018. Designing topographic heterogeneity for tidal wetland restoration. *Ecological Engineering* 123: 212–225.
- Ebberts, B.D., B.D. Zelinsky, J.P. Karnezis, C.A. Studebaker, S. Lopez-Johnston, A.M. Creason, L. Krasnow, G.E. Johnson, and R.M. Thom. 2018. Estuary ecosystem restoration: Implementing and institutionalizing adaptive management. *Restoration Ecology* 26 (2): 360–369.
- Gann, G.D., McDonald, T., Walder, B., Aronson, J., Nelson, C.R., Jonson, J., Hallett, J.G., Eisenberg, C., Guariguata, M.R., Liu, J. and Hua, F., 2019. International principles and standards for the practice of ecological restoration: Summary. *Society for Ecological Restoration*. 11 p.
- Harding, S.F., A.M. Coleman, and G.C. Roegner. 2020. Comparison of experimental and computational methods for discharge measurements from tidal wetlands. *River Research and Applications* 36 (9): 1954–1961.
- Helaire, L.T., S.A. Talke, D.A. Jay, and D. Mahedy. 2019. Historical changes in Lower Columbia River and estuary floods: A numerical study. *Journal of Geophysical Research: Oceans*, 124. <https://doi.org/10.1029/2019JC015055>
- Helaire, L.T., S.A. Talke, D.A. Jay, and H. Chang, 2020. Present and future flood hazard in the lower Columbia River Estuary: Changing flood hazards in the Portland-Vancouver Metropolitan area. *Journal of Geophysical Research: Oceans*, 125, e2019JC015928. <https://doi.org/10.1029/2019JC015928>
- Hughes, R.M., J.N. Rinne, and B. Calamusso. 2005. Historical changes in large river fish assemblages of the Americas: A synthesis. *American Fisheries Society Symposium. American Fisheries Society, Bethesda, MD* 45: 603–612.
- Hoitink, A. J. F., & D.A. Jay. 2016. Tidal river dynamics: Implications for deltas. *Reviews of Geophysics* 54(1): 240–272.
- Jay, D.A., and P. Naik. 2011. Distinguishing human and climate influences on hydrological disturbance processes in the Columbia River. *USA, Hydrological Sciences Journal* 56: 1186–1209.
- Jay, D.A., and C.A. Simenstad. 1996. Downstream effects of water withdrawal in a small, high-gradient basin: Erosion and deposition on the Skokomish River Delta. *Estuaries* 19: 501–517.
- Jay, D.A., B.S. Giese, and C.R. Sherwood. 1990. Energetics and sedimentary processes in the Columbia River Estuary. *Progress in Oceanography* 25: 157–174.
- Jay, D.A., K. Leffler, and S. Degens. 2011. Long-term evolution of Columbia River tides. *Journal of Waterway, Port, Coastal, and Ocean Engineering* 137 (4): 182–191.
- Jay, D.A., A.B. Borde, and H.L. Diefenderfer. 2016. Tidal-fluvial and estuarine processes in the Lower Columbia River: II. Water level models, floodplain wetland inundation, and system zones. *Estuaries and Coasts* 39: 1299–1324.
- Jay, D. A., K. Leffler, H.L. Diefenderfer, and A.B. Borde. 2015. Tidal-fluvial and estuarine processes in the Lower Columbia River: I. Along-channel water level variations, Pacific Ocean to Bonneville Dam. *Estuaries and Coasts* 38(2): 415–433.
- Johnson, L.K., and C.A. Simenstad. 2015. Variation in the flora and fauna of tidal freshwater forest ecosystems along the Columbia River estuary gradient: Controlling factors in the context of river flow regulation. *Estuaries and Coasts* 38 (2): 679–698.
- Johnson, G.E., G.R. Ploskey, N.K. Sather, and D.J. Teel. 2015. Residence times of juvenile salmon and steelhead in off-channel tidal freshwater habitats, Columbia River, USA. *Canadian Journal of Fisheries and Aquatic Sciences* 72 (5): 684–696.
- Ke, Y., A.M. Coleman, and H.L. Diefenderfer. 2013. Temporal land cover analysis for net ecosystem improvement. *Ecohydrology & Hydrobiology* 13 (1): 84–96.
- Kukulka, T. and D.A. Jay. 2003a. Impacts of Columbia River discharge on salmonid habitat: 1. A nonstationary fluvial tide model. *Journal of Geophysical Research* 108: 3293.
- Kukulka, T., and D.A. Jay. 2003b. Impacts of Columbia River discharge on salmonid habitat: 2. Changes in shallow-water habitat. *Journal of Geophysical Research* 108: 3294.
- Latapy, A., Y. Ferret, L. Testut, S.A. Talke, T. Aarup, F. Pons, G. Jan, E. Bradshaw, and N. Pouvreau. 2022. The data rescue process in the context of sea level reconstructions: An overview of the methodology, lessons learned, up-to-date best practices and recommendations. *Geoscience Data Journal*. <https://doi.org/10.1002/gdj3.179>
- Lichtatowich, J., R. Williams, B. Bakke, J Myron, D. Bella, B. McMillan, J. Stanford, D. Montgomery, K. Beardslee, and N. Gayeski. 2018.

- Wild Pacific salmon: A threatened legacy. Expanded July 2018 version, printed by Bemis Printing, St. Helens, OR.
- Littles, C., J. Karnezis, K. Blauvelt, A. Creason, H. Diefenderfer, G. Johnson, L. Krasnow, and P. Trask. 2022. *Adaptive management of large-scale ecosystem restoration: Increasing Certainty of habitat outcomes in the Columbia River Estuary*, e13634. USA: Restoration Ecology.
- Maier, G.O., and C.A. Simenstad. 2009. The role of marsh-derived macrodetritus to the food webs of juvenile Chinook salmon in a large altered estuary. *Estuaries and Coasts* 32 (5): 984–998.
- Marcoe, K., and S. Pilson. 2017. Habitat change in the lower Columbia River estuary, 1870–2009. *Journal of Coastal Conservation* 21 (4): 505–525.
- Matheussen, B.R., L. Kirshbaum, I.A. Goodman, G.M. O'Donnell, and D.P. Lettenmaier. 2000. Effects of land cover change on stream-flow in the interior Columbia River Basin (USA and Canada). *Hydrological Processes* 14: 867–885.
- McKeon, M., D.A. Jay, S.A. Talke, and H. Diefenderfer. 2022. Evolving sediment loads in the Columbia River Basin since the late 1800s. Submitted to *Earth Surface Processes and Landforms*.
- Miller, I.M., H. Morgan, G. Mauer, T. Newton, R. Weldon, D. Schmidt, M. Welch, and E. Grossman. 2018. Projected sea level rise for Washington State – A 2018 assessment. A collaboration of Washington Sea Grant, University of Washington Climate Impacts Group, Oregon State University, University of Washington, and US Geological Survey. Prepared for the Washington Coastal Resilience Project.
- Naik, P.K., and D.A. Jay. 2005. Virgin flow estimation of the Columbia River (1879–1928). *Hydrologic Processes* 19: 1807–1824.
- Naik, P., and D.A. Jay. 2011a. Human and climate impacts on Columbia River hydrology and salmonids. *River Research and Applications* 27: 1270–1276.
- Naik, P., and D.A. Jay. 2011b. Distinguishing human and climate impacts on Columbia River: Changes in mean flow and sediment transport. *Journal of Hydrology* 404: 259–277.
- Naiman, R.J., J.R. Alldredge, D.A. Beauchamp, P.A. Bisson, J. Congleton, C.J. Henny, N. Huntly, R. Lamberson, C. Levings, E.N. Merrill, and W.G. Pearcy. 2012. Developing a broader scientific foundation for river restoration: Columbia River food webs. *Proceedings of the National Academy of Sciences* 109 (52): 21201–21207.
- Opperman, J.J., R. Luster, B.A. McKenney, M. Roberts, and A.W. Meadows. 2010. Ecologically functional floodplains: Connectivity, flow regime, and scale 1. *Journal of the American Water Resources Association* 46 (2): 211–226.
- Palmer, M.A., Zedler, J.B., and Falk, D.A. 2016. Ecological theory and restoration ecology. In: Palmer, M.A., Zedler, J.B., Falk, D.A. (eds) Pages 3-26 in *Foundations of Restoration Ecology*. Island Press, Washington, DC. https://doi.org/10.5822/978-1-61091-698-1_1
- Pawlowicz, R., B. Beardsley, and S. Lentz. 2002. Classical tidal harmonic analysis including error estimates in MATLAB using T_TIDE *Comput. Geosci.* 28 (2002): 929–937.
- Poff, N.L., J.D. Allan, M.B. Bain, J.R. Karr, K.L. Prestegard, B.D. Richter, R.E. Sparks, and J.C. Stromberg. 1997. The natural flow regime. *BioScience* 47 (11): 769–784.
- Pulwarty, R.S., and K.T. Redmond. 1997. Climate and salmon restoration in the Columbia River Basin: The role and usability of seasonal forecasts. *Bulletin of the American Meteorological Society* 78 (3): 381–397.
- Ralston, D. K., S. Talke, W.R. Geyer, H.A.M. Al-Zubaidi, and C.K. Sommerfield. 2019. Bigger tides, less flooding: Effects of dredging on barotropic dynamics in a highly modified estuary. *Journal of Geophysical Research: Oceans* 124: 196–211. <https://doi.org/10.1029/2018JC014313>
- Roegner, G.C., E.W. Dawley, M. Russell, A. Whiting, and D.J. Teel. 2010. Juvenile salmonid use of reconnected tidal freshwater wetlands in Grays River, lower Columbia River basin. *Transactions of the American Fisheries Society* 139 (4): 1211–1232.
- Roegner, G.C., L.A. Weitkamp, and D.J. Teel. 2016. Comparative use of shallow and deepwater habitats by juvenile Pacific salmon in the Columbia River estuary prior to ocean entry. *Marine and Coastal Fisheries* 8 (1): 536–552.
- Roegner, G.C., G.E. Johnson, and A.M. Coleman. 2021. Indexing habitat opportunity for juvenile anadromous fishes in tidal-fluvial wetland systems. *Ecological Indicators* 124: 107422.
- Sather, N.K., G.E. Johnson, D.J. Teel, A.J. Storch, J.R. Skalski, and V.I. Cullinan. 2016. Shallow tidal freshwater habitats of the Columbia River: Spatial and temporal variability of fish communities and density, size, and genetic stock composition of juvenile Chinook salmon. *Transactions of the American Fisheries Society* 145 (4): 734–753.
- Scott, M.H., S.A. Talke, Jay, D.A., and Diefenderfer, H.L., 2023. Warming of the lower Columbia River, 1853 to 2018. *River Research and Applications*. <https://doi.org/10.1002/rra.4177>
- Sherwood, C.R., D.A. Jay, R.B. Harvey, P. Hamilton, and C.A. Simenstad. 1990. Historical changes in the Columbia River estuary. *Progr. Oceanogr.* 25: 299–352.
- Simenstad, C.A., D.A. Jay, and C.R. Sherwood. 1992. Impacts of watershed management on land-margin ecosystems: The Columbia River Estuary. In *Watershed Management*, ed. R.J. Naiman, 266–306. Springer-Verlag.
- Simenstad, C.A., J.L. Burke, J.E. O'Connor, C. Cannon, D.W. Heatwole, M.F. Ramirez, I.R. Waite, T.D. Counihan, and K.L. Jones. 2011. Columbia River Estuary ecosystem classification—concept and application: U.S. Geological Survey Open-File Report 2011–1228, 54 p.
- Strayer, D.L., and S.E.G. Findlay. 2010. Ecology of freshwater shore zones. *Aquatic Science* 72: 127–163.
- Talke, S. A., R. Familkhalili & D.A. Jay. 2021. The influence of channel deepening on tides, river discharge effects, and storm surge. *Journal of Geophysical Research: Oceans* 126: e2020JC016328.
- Talke, S.A., D. Mahedy, D.A. Jay, P. Lau, C. Hilley, and A. Hudson. 2020. Sea level, tidal, and river flow trends in the Lower Columbia River Estuary, 1853-present. *Journal of Geophysical Research: Oceans* 125: e2019JC015656.
- Talke, S.A., and D.A. Jay. 2013. Nineteenth century North American and Pacific tidal data: Lost or just forgotten? *Journal of Coastal Research* 29(6A): 118–127.
- Talke, S.A., and D.A. Jay. 2020. Changing tides: The role of natural and anthropogenic factors. *Annual Review of Marine Science* 12: 121–151.
- Templeton, W., and D.A. Jay. 2013. Lower Columbia River sand supply and removal: Estimates of two sand budget components. *ASCE Journal of Waterway, Port, Coastal, and Ocean Engineering* 139(5): 383–392.
- Thom, R.M., H.L. Diefenderfer, J.E. Adkins, C. Judd, M.G. Anderson, K.E. Buenau, A.B. Borde, and G.E. Johnson. 2010. Guidelines, processes and tools for coastal ecosystem restoration, with examples from the United States. *Plankton and Benthos Research* 5(Suppl.): 185–201.
- Thomas, D.W. and S.J. Bell. 1983. Changes in Columbia River estuary habitat types over the past century (Vol. 51). Astoria, Oregon: Columbia River Estuary Data Development Program.
- Tornqvist, T.E., D.J. Wallace, J.E.A. Storms, J. Wallinga, R.L. van Dam, M. Blaauw, M.S. Derksen, C.J.W. Klerks, C. Meijneken, and E.M.A. Snijders. 2008. Mississippi Delta subsidence primarily caused by compaction of Holocene strata. *Nature Geosciences* 1: 173–176.
- U.S. Army Corps of Engineers (USACE). 2010. Lower Columbia River digital terrain model: Prepared by David Smith and Associates, Inc., David Evans and Associates, Inc., and CC Patterson and

- Associates for U.S. Army Corps of Engineers, Portland District, Contract No W9127N-09-D-009, Task Order No. 0005. Available at <http://www.estuarypartnership.org/lower-columbia-digital-terrain-model>
- Waples, R.S., R.W. Zabel, M.D. Scheurell, and B.L. Sanderson. 2008. Evolutionary responses by native species to anthropogenic changes to their ecosystems: Pacific salmon in the Columbia River hydropower system. *Molecular Ecology* 17 (1): 84–96.
- Wohl, E., B.P. Bledsoe, R.B. Jacobson, N.L. Poff, S.L. Rathburn, D.M. Walters, and A.C. Wilcox. 2015. The natural sediment regime in rivers: Broadening the foundation for ecosystem management. *BioScience* 65 (4): 358–371.
- Zheng, S., B. Wu, C.R. Thorne, and A. Simon. 2014. Morphological evolution of the North Fork Toutle River following the eruption of Mount St. Helens, Washington. *Geomorphology* 208: 102–116.